

Distribution Agreement

In presenting this thesis as a partial fulfillment of the requirements for a degree from Emory University, I hereby grant to Emory University and its agents the non-exclusive license to archive, make accessible, and display my thesis in whole or in part in all forms of media, now or hereafter known, including display on the world wide web. I understand that I may select some access restrictions as part of the online submission of this thesis. I retain all ownership rights to the copyright of the thesis. I also retain the right to use in future works (such as articles or books) all or part of this thesis.

Signature:

RamoneWilliams

4.26.2010

The Effect of Curcumin Analogues on Metastasis

by

Ramone F. Williams

Department of Biology

Haian Fu, PhD
Adviser

Victor Corces, PhD
Committee Member

Barry Yedvobnick, PhD
Committee Member

04.26.2010

The Effect of Curcumin Analogues on Metastasis

by

Ramone F. Williams

An abstract of
A thesis submitted to the Faculty of Emory College of Arts and Sciences
of Emory University in partial fulfillment
of the requirements of the degree of
Bachelor of Sciences with Honors

Department of Biology

2010

ABSTRACT

The Effect of Curcumin Analogues on Metastasis

By: Ramone Williams

Tumors have often been referred to as “the wounds that never heal” because of the long suspected link between inflammation and cancer. In fact, preventable infections cause 15-20% of global cancer fatalities. The transcription factor and master regulator NF- κ B is the “missing link” between these two processes. Furthermore the effective targeting of this “common denominator” provides the rationale for the potential of the use of age-old anti-inflammatory curcumin and its analogues as a potential antimetastatic agent.

The purpose of this study was to examine the effect of novel curcumin analogues on the metastatic potential of cancer cells using a high-throughput image-based cell migration assay in a 96-well format. The high-throughput cell migration assay was developed by Platypus Technologies. The unique migration assay was utilized in conjunction with the ImageXpress5000 automated fluorescent microscope. The feasibility of the Oris™ Cell Migration Assay for the high-content screen was assessed and the imaging protocol and data analysis methods were optimized. 3,5-Bis(2-fluorobenzylidene)piperidin-4-one (EF-24) and related analogs of curcumin were tested to assess their effect on the migratory potential of cancer cells and ranked based on their potent inhibitory capabilities. The effective inhibition of the migratory potential of cancer cells may lead to the development of a new generation of novel antimetastatic drugs.

It has been found that the Oris™ Cell Migration Assay used in parallel with the IX5000 is a feasible methodology for the high-content screen. It was found that 50,000 cells/well and a 72 hour incubation-time for migration was optimal for the phenotypic image based assay. Surprisingly it was found that 20 μ M curcumin surfaced as the most potent drug when ranked based on its ability to inhibit migration in comparison to EF24 and AM- compounds.

The Effect of Curcumin Analogues on Metastasis

by

Ramone F. Williams

Advisor

Haian Fu, PhD

A thesis submitted to the Faculty of Emory College of Arts and Sciences
of Emory University in partial fulfillment
of the requirements of the degree of
Bachelor of Sciences with Honors

Department of Biology

2010

ACKNOWLEDGEMENTS

Hain Fu, PhD

Yuhon Du, PhD

Min Qui

Barry Yedvobnick, PhD

Vicotr Corces PhD

Shrikanta Chattopadhyay, MBBS

Tom Hasaka, PhD

Table Of Contents

Chapter 1: Introduction.....1

Chapter 2: Materials And Methods.....36

Chapter 3: Results And Figures.....37

Chapter 4: Discussion.....62

Chapter 5: Conclusion.....74

References.....75

Appendix.....88

LIST OF FIGURES

| | |
|----------------|----|
| Figure 1..... | 44 |
| Figure 2..... | 45 |
| Figure 3..... | 46 |
| Figure 4..... | 47 |
| Figure 5..... | 48 |
| Figure 6..... | 49 |
| Figure 7..... | 50 |
| Figure 8..... | 51 |
| Figure 9..... | 52 |
| Figure 10..... | 53 |
| Figure 11..... | 54 |
| Figure 12..... | 54 |
| Figure 13..... | 55 |
| Figure 14..... | 56 |
| Figure 15..... | 57 |
| Figure 16..... | 58 |
| Figure 17..... | 59 |
| Figure 18..... | 60 |
| Figure 19..... | 61 |

CHAPTER 1: Introduction

1.1. “Turmeric the Ancient Remedy: The Historical Uses of Curcumin”

1.1.1 Natural Drugs

Almost 61% of the approximately 877 small molecule drugs introduced globally between 1981 and 2002, were of natural origin (Goel, Kunnumakkara, & Aggarwal, 2008; Newman, Cragg, & Snader, 2003). The attention of the scientific community has been drawn to the use of such natural products in Western medicine. Most recently, emphasis has been placed on flavinoid and polyphenol plant products because of their specific biological effects on various diseases. Specifically, the ancient remedy Curcumin has emerged as multi-targeted therapeutic agent with an astounding range of beneficial properties for human health (S. Singh & Khar, 2006).

1.1.2. The Production of Turmeric and Its Plant Properties

The phenolic compound (1,7-bis(4-hydroxy-3-methoxy phenyl) -1,6-heptadiene-3,5-dione) is the active ingredient of Turmeric. Turmeric (*curcuma longa*) is a herbaceous perennial plant belonging to the Zingiberaceae or ginger botanical family native to South Asia (Mathew AG). India is the major cultivator of Turmeric producing almost 500,000 metric tons per year (Joe, Vijaykumar, & Lokesh, 2004). The plant is also produced in Bangladesh, China, Indonesia, South America, the Caribbean and in many African countries (Norman, 1991). The most prized part of the plant is the rhizome, the underground stem from which the tuberous roots and shoot grow. This valued portion is

known as finger Turmeric, it is boiled, drained, crushed and dried into a yellow powder that has been used as a cosmetic, fabric dye, spice, and herbal remedy for over 2000 years (Mathew AG; Thomas-Eapen, 2009).

1.1.3. The Use of Turmeric in Cosmetics and Textiles

Cosmetically, Turmeric has been used traditionally in perfumes as well as for skin health. Turmeric paste is applied as a mask to the face and skin to improve appearance and to fade blemishes (Hatcher, Planalp, Cho, Torti, & Torti, 2008; Thomas-Eapen, 2009). In Turkey, Henna-natural henna set (red) contains turmeric and other ingredients to vary hair color. Other cosmetics include balms creams and oils in Thailand, Japanese soaps and lotions in both Japan and the US (Goel, Jhurani, & Aggarwal, 2008). In textiles, Turmeric is used as a vibrant yellow dye. The dyed material is often incorporated as an integral part of weddings and religious ceremonies and is considered favorably by most in Indian culture (Thomas-Eapen, 2009).

1.1.4. Turmeric as a Spice

Turmeric is used extensively in South Asian cuisine. The spice, a major ingredient in many curry powders, is used sparingly to give a flavorsome taste to meat, fish, vegetable, beans and lentils. In the 14th century, the spice was brought to the Western world from Asia by early European explorers and is used today in mustards and sauces (S. Shishodia, Sethi, & Aggarwal, 2005; Thomas-Eapen, 2009; Tilak, Banerjee, Mohan, & Devasagayam, 2004). Turmeric is also used as a flavoring in cheese, butter and other foods (H. P. Ammon & M. A. Wahl, 1991; Goel, Kunnumakkara, et al., 2008;

Govindarajan, 1980). Turmeric colorant is used to provide bright hues in the food industry, and natural green color is made from turmeric and vegetable juice. Other products include goat milk with curcumin from China, desserts such as lemon sponge pudding, Alpro vanilla flavored soya dessert and Alpro custard, in the UK and Longley Farm vanilla yogurt in the US (Goel, Jhurani, et al., 2008). Interestingly aside from its zest, Indians often add a pinch of the seasoning to most of their cuisine because of the Ayurvedic principle affirming healing properties it possesses (Thomas-Eapen, 2009).

1.1.5. Turmeric's Age-Old Healing Properties

Turmeric's value as a medicinal compound dates back to 2000BC. It was part of Ayurveda, the ancient Indian system of holistic medicine centered on plant based drugs. Turmeric has been documented as a treatment for dental diseases, liver disorders, digestive disorders, anorexia, rheumatism, diabetic wounds, runny nose, sinusitis and to ease the hallucinatory effects of psychotropic drugs (Araujo, 2001; Goel, Kunnumakkara, et al., 2008; Hatcher, et al., 2008; Tilak, et al., 2004). In a warm moist preparation, Turmeric paste is used to dress wounds and to treat infections, bites, burns, acne, and various skin diseases (Hatcher, et al., 2008; Thakur, 1989). In fact, for the Indian market Johnson & Johnson manufactures Turmeric Band-Aids known colloquially as "Band-Aid *Haldi*" (Hatcher, et al., 2008; MacGregor, 2006). The poultice is also used during childbirth to heal any lacerations to the birth canal. After childbirth women are given a tonic containing Turmeric paste to drink two times a day (Hatcher, et al., 2008; Pandeya, 2005). Likewise, powdered Turmeric is used to cure respiratory ailments and roasted Turmeric is used as antidiysenteric for children (Hatcher, et al., 2008; Thakur, 1989). The

use of curcumin, specifically an anti-inflammatory, has prevailed in cultures beyond Hindu medicine including traditional Chinese medicine and in age-old remedies throughout the Orient (Goel, Kunnumakkara, et al., 2008). Conceding the recent emphasis of the use of complementary and alternative medicines such as curcumin in Western medicine, modern scientific studies over the past half century have validated the therapeutic effects of this time-honored remedy (Goel, Kunnumakkara, et al., 2008).

1.2.“CUREcumin: The Modern-Day Multi-Targeted Miracle Drug”

1.2.1. The Discovery and Isolation of Curcumin

In 1815, Curcumin was first isolated and was subsequently crystallized in 1870 (Daybe, 1870). The compound was eventually identified as 1,6-heptadiene- 3,5-dione- 1,7-bis(4-hydroxy-3-methoxyphenyl)-(1E,6E) or diferuloylmethane. It was not until 1910 that the feruloylmethane skeleton of curcumin was synthesized and confirmed by Lampe and Milobedeska (Goel, Jhurani, et al., 2008; Goel, Kunnumakkara, et al., 2008; Milobedzka, 1910).

Usually extracts of *Curcuma longa* or Turmeric contain three structures known as “the curcumin complex” “the curcumins,” or the “the curcuminoids.” This complex consists of the trio curcumin (curcumin I), demethoxycurcumin (curcumin II), and bisdemethoxy curcumin (curcumin III); of which curcumin I the active principle predominates. Curcumins make up between one and six percent of powdered Turmeric and other natural derivatives constitute a maximum three percent. Curcumin is extracted from Turmeric using ethanol or other organic solvents (Kidd, 2009).

1.2.2. The Chemical Properties of Curcumin

The yellow-orange powder is insoluble in water and ether but exhibits slight solubility in ethanol and methanol, and good solubility in dimethylsulfoxide, chloroform and acetone (Goel, Kunnumakkara, et al., 2008; Hatcher, et al., 2008; Payton, Sandusky, & Alworth, 2007). Curcumin’s molecular formula is $C_{21}H_{20}O_6$ with a molecular weight of 368.37g/mol. Its melting point is 183°C. Curcumin is lipophilic and mimics apoptotic

events by disrupting cell membranes (Hatcher, et al., 2008; Holder, Plummer, & Ryan, 1978). In spectroscopy, the maximum absorption λ_{max} of curcumin in methanol occurs at 430nm, and at a value between 415-420nm in acetone (B. B. Aggarwal, Kumar, & Bharti, 2003; Goel, Kunnumakkara, et al., 2008). At pH 2.5-7 curcumin displays a brilliant yellow color and appears red at pH >7 (Goel, Kunnumakkara, et al., 2008). Curcumin exists in both β -diketone and enol-tautomer forms (Goel, Kunnumakkara, et al., 2008). Existing primarily in its enolic form, its enolic proton has a pKa of approximately 8.5 and its two phenolic protons have pKas between 10 and 10.5. All three protons are ionizable in water (Hatcher, et al., 2008).

Curcumin is most stable at acidic pH. For example curcumin degradation is extremely slow at the pH typically encountered in the stomach, specifically pH 1-6. On the contrary, at basic pH curcumin is unstable and degrades to ferulic acid and feruloylmethane. For example, after 30 minutes of placement in phosphate buffer systems of pH 7.2, greater than 90% of curcumin was rapidly degraded (Goel, Kunnumakkara, et al., 2008; Oetari, Sudiby, Commandeur, Samhoedi, & Vermeulen, 1996; Y. J. Wang et al., 1997). In contrast, in cell culture medium containing 10% fetal bovine serum or in human blood, curcumin is quite stable – greater than 20% is degraded after 1 hour and approximate 50% after 8 hours (Goel, Kunnumakkara, et al., 2008; Y. J. Wang, et al., 1997). Studies have identified intestinal metabolites in humans and rats, including curcumin glucuronide, curcumin sulfate, tetrahydrocurcumin and hexahydrocurcumin. These metabolites were found upon oral administration of curcumin in rats – indicating that such decomposition productions of curcumin are present in vivo and may play a role in biological activity (Hatcher, et al., 2008; Holder, et al., 1978; Ireson et al., 2002).

1.2.3. Curcumin's Vast Range of Targets

Conceding curcumin's complex chemistry, the polyphenol is a remarkably pleiotropic molecule affecting a myriad of biochemical and molecular cascades through its vast range of molecular targets. Curcumin's targets include enzymes, transcription factors, cell proliferation and apoptosis regulating genes, growth factors and their receptors, cytokines, metals, albumin and other molecules (Goel, Kunnumakkara, et al., 2008).

1.2.4. The Biological Effects and Therapeutic Roles of Curcumin

Curcumin's biological effects are as wide ranging as its molecular targets (Goel, Kunnumakkara, et al., 2008; Hatcher, et al., 2008; S. Singh & Khar, 2006). Extensive preclinical studies have characterized curcumin as hepatoprotective (Kiso, Suzuki, Watanabe, Oshima, & Hikino, 1983), thrombosuppressive (Srivastava R, 1985), cardiovascular – exhibiting protection against myocardial infarction (Dikshit, Rastogi, Shukla, & Srimal, 1995; Nirmala & Puvanakrishnan, 1996; Venkatesan, 1998) , hypoglycemic (Srinivasan, 1972), antiarthritic – exhibiting protection against rheumatoid arthritis (Deodhar, Sethi, & Srimal, 1980), antimicrobial in *Helicobacter pylori* infection (De et al., 2009) and an HIV an anti-viral agent. (Kutluay, Doroghazi, Roemer, & Triezenberg, 2008).

In addition clinical trials suggest a possible therapeutic role for curcumin in diseases such as familial adenomatous polyposis (Cruz-Correa et al., 2006), Chron's disease and ulcerative proctitis (187), gall bladder disease (178,179), inflammatory bowel disease (Garcea et al., 2004; Holt, Katz, & Kirshoff, 2005), ulcerative colitis (Garcea, et

al., 2004), hypercholesteremia, atherosclerosis (Soni & Kuttan, 1992), pancreatitis (Durgaprasad, Pai, Vasanthkumar, Alvres, & Namitha, 2005), psoriasis (Heng, Song, Harker, & Heng, 2000), external sebaceous neoplasms (Kuttan, Sudheeran, & Josph, 1987), chronic anterior uveitis (Lal et al., 1999), idiopathic inflammatory orbital pseudotumors (Lal, Kapoor, Agrawal, Asthana, & Srimal, 2000) (Goel, Kunnumakkara, et al., 2008), multiple myeloma (Xiao, Xiao, Zhang, Zuo, & Shrestha, 2010), myelodysplastic syndromes (Hatcher, et al., 2008), Alzheimer's disease (Ma et al., 2009), cystic fibrosis (Cartiera et al., 2010), and multiple sclerosis (Chearwae & Bright, 2008) (Hatcher, et al., 2008).

1.2.5. Cucumin's Multi-Targeted Effects on Cancer

Most important are curcumin's multitargeted effects on cancer (Goel, Kunnumakkara, et al., 2008; Hatcher, et al., 2008; S. Singh & Khar, 2006). Such functions include its role as an antioxidant – capable of inducing apoptosis (Sreejayan & Rao, 1997), antiproliferative (Mehta, Pantazis, McQueen, & Aggarwal, 1997), anti-inflammatory (H. P. T. Ammon & M. A. Wahl, 1991; Deodhar, et al., 1980; Dikshit, et al., 1995), radiosensitizing, radioprotective (Chendil, Ranga, Meigooni, Sathishkumar, & Ahmed, 2004; Jagetia, 2007; Li, Zhang, Hill, Wang, & Zhang, 2007), anti mutagenic (Shukla, Arora, & Taneja, 2002), antiproliferative (Mehta, et al., 1997), anti-cancer (Sun, Liu, Chen, & Liu, 2005), anticarcinogenic (Kiso, et al., 1983; Limtrakul, Lipigorngoson, Namwong, Apisariyakul, & Dunn, 1997; Rao, Rivenson, Simi, & Reddy, 1995), chemotherapeutic (Lopez-Lazaro, 2008), chemopreventative (Maheshwari, Singh, Gaddipati, & Srimal, 2006) chemosensitizing (Chirnomas et al., 2006; Garg, Buchholz, &

Aggarwal, 2005), antitumoral (Azuine & Bhide, 1992; Deshpande, Ingle, & Maru, 1997; S. V. Singh et al., 1998), antiangiogenic (Arbiser et al., 1998), anti-invasive and antimetastatic agent (Menon, Kuttan, & Kuttan, 1995; Santibanez, Quintanilla, & Martinez, 2000; Stetler-Stevenson, 1999).

1.2.6. The Coining of the Nickname “CUREcumin”

Conceding the astonishing breadth of the aforementioned therapeutic effects of curcumin, the extraordinary scope and latitude of curcumin’s beneficial properties has earned this miracle molecule the nickname “CUREcumin” (Goel, Kunnumakkara, et al., 2008). The need for such a multi-target based drug is imperative for the treatment of complex human disease. Most relevant to this study is curcumin’s potential as robust therapeutic for the intricacies of tumor progression in cancer, specifically in metastasis. Moreover, no toxicity in curcumin has been discovered to date, even at very high doses in either animal or human studies (Lao et al., 2006; Qureshi, Shah, & Ageel, 1992; Shankar, Shantha, Ramesh, Murthy, & Murthy, 1980). Not to mention, curcumin’s low-cost addresses the issue presented by the large number of effective drugs beyond the reach of the majority of the population due to their high-cost (Goel, Jhurani, et al., 2008)

1.2.7. Curcumin’s Major Mechanism of Action: Its Role as a Free Radical Scavenger

A variety of different mechanisms mediate curcumin’s biological effects. The most significant mechanism responsible for virtually all of curcumin’s properties is its function as a scavenger of reactive oxygen and nitrogen free radicals (Das & Das, 2002;

Priyadarsini, 1997). This ability to scavenge free radicals can either arise from the phenolic OH group or from the CH₂ group of the β-diketone. It has been shown by several groups that curcumin's activity is due primarily to its phenolic OH (Priyadarsini et al., 2003; Vajragupta et al., 2003)

Reactive oxygen species (ROS) are reactive molecules containing the oxygen atom including superoxide anion (O₂⁻), hydrogen peroxide (H₂O₂), singlet oxygen (O), hydroxyl radical (OH) and peroxy radical (OOH). Under environmental stress such as UV or heat exposure, ROS levels significantly increase, which can result in cell structure injury. Glutathione (GSH) is the fundamental ROS defense system in the cells. GSH levels increase with ROS levels during apoptosis (Chandra, Samali, & Orrenius, 2000; Syng-Ai, Kumari, & Khar, 2004). Glutathione-S-transferase regenerates GSH. When targeted by curcumin, ROS production and cytochrome c release are induced in AK-5 cells resulting in apoptosis (Bhaumik, Anjum, Rangaraj, Pardhasaradhi, & Khar, 1999).

Fascinatingly, curcumin's redox profile is quite intricate. In fact, curcumin has been shown to also inhibit ROS production in apoptosis (Somasundaram et al., 2002) and to increase GSH content in UV and glucocorticoid treated cells (Piwocka, Jaruga, Skierski, Gradzka, & Sikora, 2001). In the same way this complexity affects curcumin's effect on the permeability transition pore (PTP) in the mitochondria. Curcumin induces PTP opening at a concentration of 20 μM while higher concentrations inhibit opening under differing experimental conditions.

Curcumin's redox properties are executed at the transcriptional level also (Balogun et al., 2003). Haemoxygenase-1 (HO-1) is an inducible redox-sensitive ubiquitous protein that degrades heme to CO. It is well documented that curcumin has

been shown to protect cells from oxidative stress by upregulating HO-1 in the endothelium (Motterlini, Foresti, Bassi, & Green, 2000). Curcumin enables the translocation of transcription factor Nrf2 to the nucleus. Nrf2 is subsequently able to initiate the transcription of cryprotective proteins and detoxifying enzymes by binding to the anti-oxidant responsive element (Balogun, et al., 2003).

The most relevant example of curcumin's free radical scavenging activity involves cyclooxygenase (COX) and lipoxygenase (LOX) which modulate tumor growth and cell proliferation, tumor cell adhesion and metastatic potential respectively (Honn et al., 1989; Marnett, 1992). The biosynthesis of COX and LOX metabolites are associated with arachidonic acid metabolism implicates ROS and other free radicals. It is not surprising then that curcumin inhibits both COX and LOX activity and arachidonic acid metabolism (Beg & Baltimore, 1996).

1.2.8. Curcumin's Major Biological Role as an Anti-Inflammatory

In ancient medicine, curcumin's usage has been primarily applied to the treatment of inflammatory disease. Curcumin inhibits various signaling pathways and consequently elicits a holistic anti-inflammatory response. Likewise there is evidence suggesting possible therapeutic uses in a plethora of diseases mediated by inflammatory processes.

For example, curcumin has been shown to inhibit the transcription of macrophage inflammatory protein-2 (MIP-2). MIP-2 plays a key role in various inflammatory states of the central nervous system such as traumatic brain injury and experimental allergic encephalitis the animal model for multiple sclerosis (Tomita, Holman, Santoro, & Santoro, 2005). Curcumin's inhibition of COX-2 expression provides a rationale for its

application in the treatment of the COX-2 induced inflammation resulting from non melanoma skin cancer (Cho et al., 2005; Granstein & Matsui, 2004). In haline membrane disease (HMD) and diniotrobenzene sulfonic acid induced colitis curcumin has been implicated in regulating the pro-inflammatory cytokine expression (Literat et al., 2001; Salh et al., 2003). Curcumin has also been show to supress the degranulation and activation of mast cells – key regulators of inflammation the produce neutral protease, histamine and proinflammatory cytokines. Curucmin also targets the induction of NO sythase and the gene expressing monocyte chemoattractant protein 1 both mediators of the inflammatory process (Chao, Hu, Molitor, Shaskan, & Peterson, 1992; Fischer & Reichmann, 2001; H. Y. Kim, Park, Joe, & Jou, 2003)

Curcumin's potent anti-inflammatory activity arises primarily from its ability to inhibit the transcription factor NF- κ B. In hemorrhagic shock, curcumin decreases liver injury by inhibiting both NF- κ B and AP-1. Similarly curcumin has been show to inhibit liver inflammation and hyperplaxia through a mechanism targeting NF- κ B as well (Beasley, Hwang, Lin, & Chien, 1981; Gaddipati et al., 2003).

Curcumin's inhibition of NF- κ B extends considerably beyond the scope of the aforementioned examples. Fascinatingly, NF- κ B plays a crucial role not only in signal transduction pathways involved in inflammatory disease, but also in numerous cancers. The role of viral, bacterial, or chemically induced chronic inflammation in carcinogenesis has been widely recognized and will be discussed in depth in the following chapter ((Amit & Ben-Neriah, 2003; Baeuerle & Henkel, 1994; Barnes & Karin, 1997; Siebenlist, Franzoso, & Brown, 1994)

1.3. “Band-Aid *Haldi* for the Wound That Never Heals: Curcumin’s Role in the Connection between Cancer and Inflammation”

1.3.1. The Connection between Cancer and Inflammation

The connection between inflammation and carcinogenesis has long been known but the precise mechanisms have yet to be elucidated (Naugler & Karin, 2008). Interestingly, tumors have long been referred to as “wounds that never heal” (Balkwill & Mantovani, 2001; Dvorak, 1986). In 1986 Dvorak paralleled wound healing and tumor stroma formation (Balkwill & Mantovani, 2001). What's more, angiogenesis, cell motility and the activation of matrix remodeling are all common features shared by inflammation and carcinogenesis (Novak).

In 1863 Rudolf Virchow, the time-honored pathologist, first deduced the notion that inflammation may support or promote cancer after observing the presence of leukocytes in neoplastic tissue (Balkwill & Mantovani, 2001; Naugler & Karin, 2008). Over a century later this concept has since resurfaced and has been investigated and supported in modern studies. It has been found not only that chronic infections trigger 15% of cancer occurrences worldwide, but also that preventable infections cause 15-20% of global cancer fatalities (Kuper, Adami, & Trichopoulos, 2000). Similarly, chronic inflammation resulting from chemicals, physical agents and autoimmune reactions increases the risk of cancer and hastens its progression (Gulumian, 1999; Karin, 2006b). In target cells ROS and particular cytokines are produced in inflamed tissues causing DNA damage. The survival of these damaged cells potentially lead to neoplastic transformation (Calmels, Hainaut, & Ohshima, 1997).

In wounds, platelets are not only a vital source of cytokines, but are also key in tumor angiogenesis (Pinedo, Verheul, D'Amato, & Folkman, 1998). In the same way, cancerous cells secrete proinflammatory cytokines such as TNF- α , IL-1, IL-6 and several different chemokines (Burke, Relf, Negus, & Balkwill, 1996). However, wound-healing is usually self-limiting, while in tumor progression the secretion of VEGF induces constitutive extravasation of fibrin and fibronectin as well as continuous generation of extracellular matrix. In a comparative assessment of wounds and tumors using gene-expression-profiling analysis, it was found that a wound-response gene-expression pattern could predict the likelihood of metastasis and survival in breast cancer patients (Adler et al., 2006).

Further evidence strengthening the link between inflammation and carcinogenesis is the composition of the tumor microenvironment. The tumor microenvironment is characterized by the presence of inflammatory cells localized in both the tumor itself and the stroma (Negus, Stamp, Hadley, & Balkwill, 1997). Tumor associated macrophages (TAMs) are a major component of the infiltrate of almost all tumors (Mantovani, Bottazzi, Colotta, Sozzani, & Ruco, 1992). TAMs stimulate tumor cell proliferation, angiogenesis and metastasis (Mantovani, Bussolino, & Dejana, 1992). In the same way, tumor associated dendritic cells (TADC) and tumor-infiltrating T cells (TIL) are both characterized by defective responses to tumor antigens (Allavena et al., 2000; Mizoguchi et al., 1992). On a whole, the presence of these inflammatory cells influence cancer growth, carcinogenesis associated with immunosuppression and most importantly metastasis (Balkwill & Mantovani, 2001).

1.3.2. NF- κ B the Common Denominator

NF- κ B serves as master regulator of inflammation and furthermore has been implicated in every single hallmark of cancer. Consequently, it is not surprising that NF- κ B is indeed the missing link in long suspected connection between inflammation and carcinogenesis (Naugler & Karin, 2008). Nuclear Factor Kappa B transcription factors play a significant role in the integration of multiple stress stimuli and in mediating immune responses in inflammatory states. Additionally, constitutively activated NF- κ B has been implicated in all six of the essential alterations required in tumorigenesis: self-sufficiency in growth signals; insensitivity to growth inhibition; evasion of apoptosis immortalization; sustained angiogenesis; and tissue invasion and metastasis (Hanahan & Weinberg, 2000). Thus one can easily see why NF- κ B was the obvious culprit in the case of determining the common denominator.

“NF- κ B” is in fact a misnomer, first discovered in the nuclei of B cells as a protein bound to the kappa immunoglobulin gene enhancer. In actuality, NF- κ B generally resides in the cytoplasm in its inactive state (Sen & Baltimore, 1986). The transcription factor is a hodgepodge of closely related protein dimers that come together to form various homo and hetero- dimers able to bind the κ B sequence motif.

The medley of proteins includes five reticulendotheliosis family (REL) proteins belonging to two classes distinguished by their mode of synthesis and transcriptional activation properties. RELA (p65), RELB and c-REL do not require processing as they are synthesized in their mature forms. This class of proteins is also characterized by their possession of REL homology domains or RHDs which facilitate DNA binding and dimerization. Proteins also possess transcription modulating domains at their carboxy

terminus. The second class of proteins consists of NF- κ B1 (p105), NF- κ B2 (p100). Their final form is characterized by the presence of RHD but the absence of transcription-modulating domains. Initially NF- κ B1 and NF- κ B2 are secreted as precursor proteins with an N terminal RHD and a C-terminal repeating sequences of 30-33 amino acids found in the ankyrin protein. The C-terminal domain is removed by ubiquitin-dependent proteolytic processing resulting in the final product (Ghosh, May, & Kopp, 1998; Karin, Cao, Greten, & Li, 2002).

NF- κ B is usually regulated by two pathways: the canonical and the non-canonical pathway. The canonical pathway involves dimers composed of RELA, c-REL and p50. The pathway is dependent on NEMO/IKK β activation and is normally triggered in response to microbial and viral infection as well as exposure to proinflammatory cytokines (Balkwill & Mantovani, 2001). The non-canonical pathway involves the NF- κ B2 and RELB dimer. It is dependent on IKK α activation via upstream NIK and is triggered by members of the TNF cytokine family (Karin, et al., 2002; Naugler & Karin, 2008; Senftleben et al., 2001; Solan, Miyoshi, Carmona, Bren, & Paya, 2002).

Both pathways involve the phosphorylation- and ubiquitin-dependent proteolytic removal by the 26S proteasome of I κ B – the protein inhibitor that holds NF- κ B hostage in the cytoplasm. I κ B is composed of two catalytic subunits (IKK α and IKK β) and one regulatory (IKK γ /NEMO) subunit. This elimination of I κ B liberates NF- κ B and permits its translocation into the nucleus allowing transcription of its target genes which can be divided into four functional categories; immunoregulatory, inflammatory, antiapoptotic and genes that encode negative regulators of NF- κ B. Aberrant activation contributes to

deregulated growth, resistance to apoptosis and importantly tendency to metastasize (Kasinski et al., 2008).

Activation of NF- κ B has been observed in but is not limited to breast (Chua et al., 2007), lung (16), colon (Scartozzi et al., 2007) and, pancreatic (Annunziata et al., 2007) cancers, melanoma (Yang, Pan, Clawson, & Richmond, 2007), multiple myeloma (Annunziata, et al., 2007) , several types of leukemia (Fabre et al., 2007; Rae, Langa, Tucker, & MacEwan, 2007; Vilimas et al., 2007) and lymphoma (Fabre, et al., 2007; Zou, Kawada, Pesnicak, & Cohen, 2007). With the advent of advanced experimental mouse models of cancer, specific functions of NF- κ B activation has been tied to the activation carcinogenesis, tumor progression and notably metastogenesis. Fundamental to this study is NF- κ B's specific role in metastasis which will be elucidated in the following chapter.

1.3.3. NF- κ B as a Target of Curcumin

The common denominator, NF- κ B is one of curcumin's numerous targets further validating the notion for use of the age-old anti-inflammatory curcumin as an effective anti-cancer agent.

It is well documented that curcumin inhibits TNF-, phorbol ester-, and hydrogen peroxide- dependent activation of NF- κ B, possibly by quenching the reactive oxygen intermediates produced by all three inducers (Sanjaya Singh & Aggarwal, 1995). Curcumin is also able to suppress downstream products of NF- κ B. For example COX-2, a target previously discussed, has also been suppressed in rat peritoneal platelets (H. P. Ammon & M. A. Wahl, 1991), in mouse epidermis (Huang et al., 1991), in

gastrointestinal cell lines and in human colon epithelial cells (Plummer et al., 1999). Similarly, Cyclin D1 was downregulated by curcumin in human multiple myeloma (MM) cells (A. C. Bharti, N. Donato, S. Singh, & B. B. Aggarwal, 2003), HUVECs (Park et al., 2002), prostate and breast cancer in cell culture resulting in an inhibition of proliferation (Mukhopadhyay et al., 2002) in rat hepatic stellate cells in a model of chronic liver disease (Y. Cheng, Ping, & Xu, 2007). In the same way curcumin suppresses Bcl-2 and Bcl-X_L anti-apoptotic proteins. Curcumin inhibited the constitutive expression of Bcl-2 and Bcl-X_L induced apoptosis in human MM cells (Alok C. Bharti, Nicholas Donato, Sujay Singh, & Bharat B. Aggarwal, 2003) and human mantle cell lymphoma (MCL) – an aggressive B cell non-Hodgkin's lymphoma (Shishir Shishodia, Amin, Lai, & Aggarwal, 2005). Curcumin also inhibits several cytokines including IL-1, -2, -6, -8, and -12, TNF, and interferon- γ (IFN- γ) which can be attributed to its blockade of NF- κ B (Bhattacharyya et al., 2007; Cho, Lee, & Kim, 2007; Gao et al., 2004; Hidaka et al., 2002; Xu, 1998).

1.3.4. TNF α a Crucial Target Gene of NF- κ B

TNF is one of the most important target genes of NF- κ B. Upon activation, NF- κ B upregulates TNF which sequentially upregulates IL-1. It has been well documented that the two proinflammatory cytokines potentiate the production of each other. Furthermore, these cytokines possess astonishing pleiotropic character with the ability to induce acute or chronic inflammation in most if not all tissues and organ systems in the body.

1.4. “The Antimetastatic Effects of the Ancient Anti-Inflammatory”

1.4.1. The Complex Process of Metastasis

In the early days, metastasis was defined as the transportation of any substance, whether metal or coal dust, normal cells (placenta, bone marrow), bacteria, or cancer cells from one part of the organism to another. Yon Recklinghausen was the first to restrict the definition to the transport of pathological substances. Around 1913 the definition was limited further to describe secondary tumor nodules that occurred frequently in cancer (Levin, 1913).

Metastasis is a complex multi-step process. These steps include: tumor cell mobilization, intravasation of the tumor vasculature and extravasation at secondary sites (Baumann, 2008). This study focuses on lung cancer.

Lung cancer is the most common cause of cancer-related death in both men and women; it is also the second most common cancer in the United States ("A Snapshot of Lung Cancer," 2009) Metastasis occurs in approximately 30%-40% of all lung cancer cases and most often spreads to the liver, adrenal glands, bones, and brain ("What You Need to Know About Lung Cancer," 2007)

1.4.2. Nf- κ B and Metastasis

Nf- κ B, the missing link between inflammation and carcinogenesis, is in all likelihood the *raison d'être* for the anti-cancer activity of the anti-inflammatory curcumin. Arguably, the most striking similarities between wound-healing and cancer is during late

stage of tumor progression – particularly during metastasis. Its role in this complex multi-step process is pivotal to this work.

The Epithelial to Mesenchymal Transition (EMT) is a program of development involving a loss of cell-cell adhesion, apical-basolateral polarity, and epithelial markers, and a concurrent gain in spindle-cell shape, mesenchymal markers and most importantly motility. Though still controversial whether metastasis truly represents an EMT, this term has been more generally employed to mean identifiable change in cellular phenotype characterized as loss of cell junctions and an acquisition of migratory behaviors in cancer (Cowin & Welch, 2007; Tsuji, Ibaragi, & Hu, 2009). In recent studies, canonical activation of Nf- κ B has been implicated in this process (Huber et al., 2004; Naugler & Karin, 2008). In a model of breast cancer Nf- κ B was found to mediate the activation of the mesenchymal program which involves the genes: MM2/9, VACM-1, ICAM-1 and Cathepsins B and Z (Basseres & Baldwin, 2006; Naugler & Karin, 2008). Importantly, a reversal of EMT was observed upon the inhibition of Nf- κ B.

EMT is also characterized by the repression of E-cadherin whose expression has been newly implicated in Nf- κ B regulation. It was found that Nf- κ B's repression of E-cadherin in breast cancer boosts EMT (Chua, et al., 2007). In the same way, Nf- κ B activation of Bcl2 in breast cancer (X. Wang et al., 2007) have been shown to promote EMT as well. Likewise, It has been well documented that Nf- κ B induction of the transcription factor TWIST (Horikawa et al., 2007; Yang et al., 2004) has produced a more malignant and metastatic phenotype. Furthermore, in prostate cancer IKK α activation represses expression of mpsin, the metastasis suppressor gene. In IKK α

mutant tumors, a knockdown of mmp13 expression re-establishes metastatic potential (Luo et al., 2007; Naugler & Karin, 2008).

1.4.3. Curcumin Inhibits Metastasis In-Vitro and In-Vivo

Considering Nf- κ B's paramount role in metastasis, there are several examples of curcumin's antimetastatic potential both in-vitro and in-vivo. Curcumin suppressed Nf- κ B activation in human colorectal cancer (CRC) in nude mice. Ascites and distant metastases to the liver, intestines, lungs, rectum and spleen were inhibited in the orthotopic mouse model. Additionally, western blot and immunohistochemical analysis revealed that curcumin decreased the expression of genes involved in invasion (MMP-9 and ICAM-1) and metastasis (CXCR4) expression (Kunnumakkara et al., 2009).

Similarly, In U937 (human myeloid leukemia) and A293 (human embryonic kidney) cell lines, curcumin has been shown to inhibit Nf- κ B activation. Suppression of the activation of Nf- κ B mediated gene expression of metastasis promoting genes including VEGF, MMP-9, ICAM-1, through inhibition of IKK and Akt was also evident (S. Aggarwal et al., 2006). Lastly, curcumin was shown to have an Nf- κ B mediated anti-metastatic effect in the highly invasive MDA-MB-231 breast cancer cell line (Bachmeier et al., 2007).

1.4.4. Curcumin's Inhibition of Metastasis through Cellular Adhesion Molecules

Yet another way in which Curcumin is able to inhibit metastasis, is by targeting cellular adhesion molecules. Cellular adhesion molecules or CAMs are proteins located on the surface of the cell that mediate binding with the extracellular matrix or with other

cells. (Bhandarkar & Arbiser, 2007). Curcumin's targeting of CAMs at the transcriptional level was revealed in the previous section. Specifically, curcumin regulates intracellular adhesion molecule (ICAM-1), endothelial leukocyte adhesion molecule-1 (ELAM-1) and vascular cell adhesion molecule-1 (VCAM-1). ICAM-1 and VCAM-1 both carry a different number of extracellular immunoglobulin (Ig)-like domains and thus are members of the Ig gene superfamily (Kobayashi, Boelte, & Lin, 2007; Lee & Benveniste, 1999). The cell surface expression of all three CAMs are inhibited and consequently prevent the adhesion of monocytes to endothelial cells (Thaloor et al., 1998).

Bringing this discussion full circle, curcumin's inhibition of CAM's further elucidates the link between inflammation and cancer. CAMs are implicated not only in metastasis but also upon the onset of inflammation (Kobayashi, et al., 2007; Zetter, 1993). Specifically, during intravasation in metastasis, cancer cells from the primary site cross the basement membrane and vascular endothelium to reach the blood circulation for dispersal to target organs. During extravasation the cells bind to the inflamed vascular endothelium through CAMs and later migrate across the endothelium to the tissue to establish new growth at preferential sites (Kobayashi, et al., 2007). In the same way, during inflammatory processes, leukocytes migrate to sites of injury or infection. Cells successively interact with ICAM-1 and VCAM-1 on the activated vascular epithelium. Cells roll along the endothelial surface until securely adhered and then extravasate to the target tissues (Ebnet & Vestweber, 1999).

1.5. “The Problem: The Poor Bioavailability of Curcumin; The Answer: Analogues”

1.5.1. Curcumin’s Poor Bioavailability

Curcumin’s astonishing range of targets is fundamental to its characterization as a modern day miracle drug. Ironically, even at extremely high doses curcumin exhibits its poor bioavailability in target organs within the body (Goel, Jhurani, et al., 2008). The issue of bioavailability is one of several deemed central to the efficacy of a course of therapy. In 1978 Wahlstrom and Blennow were the first to examine the pharmacokinetics of curcumin. Curcumin was orally administered at 1g/kg to rats. It was found that approximately 75% of ingested curcumin was excreted in the feces and negligible amounts were found in the urine. Moreover, it was determined that curcumin was poorly absorbed from the gut. Even after doses up to 5g/kg, no toxicity was detected. Upon intravenous injection curcumin was actively transported into the bile, but the major part of the drug was metabolized. On the whole this data suggested poor absorption and rapid metabolism of curcumin (Wahlstrom & Blennow, 1978). Similarly, studies investigated the amount of curcumin in human tissue. It was found that the bioavailability of curcumin is poor in tissues distant from the gastrointestinal tract including the liver (Garcea, et al., 2004). In other studies it was suggested that a daily dose of 1.6g of curcumin is needed for effectiveness in humans (Sharma et al., 2001).

In attempts to circumvent these issues of poor bioavailability, further studies used very high doses of curcumin. Nonetheless, the percentage of curcumin absorbed remained constant between 60 and 66% of the administered dose. Absorption did not

increase with further dosage increase (Pan, Huang, & Lin, 1999; Ravindranath & Chandrasekhara, 1980, 1981). In a phase I trial of patients with high-risk or premalignant lesions curcumin was administered orally ranging from 500 to 8000 mg/day for 3 months. No toxicity was found at any single dose. At doses lower than 4000 mg/day, curcumin was not detected in the serum, at 4000 mg/day the maximum serum concentration ranged from $0.5 \pm 0.11 \mu\text{M}$ and at 8000 mg/day, $1.77 \pm 1.87 \mu\text{M}$ (A. L. Cheng et al., 2001).

A second elegant dose escalation trial involving healthy volunteers administered doses of curcumin ranging from 500 to 12,000 mg. Findings were similar to Cheng *et al.* (A. L. Cheng, et al., 2001). No toxicity was detected and the presence of curcumin in the serum could only be detected at the uppermost dosages between 10,000 and 12,000 mg/day. Additionally, more than three different phase I clinical trials document that curcumin at doses as high as 12g/day is well tolerated (Ravindranath & Chandrasekhara, 1980; Shoba et al., 1998). All these studies are a testament to curcumin's extraordinary safety profile. Furthermore the average daily intake of turmeric in the Indian diet is between 2 and 2.5g for a 60kg individual. This day by day dietary intake is equivalent to a dosage of 60-100 mg of curcumin and may be responsible for the lower incidence of cancer in the Indian population (Goel, Jhurani, et al., 2008).

In Cheng *et al.* it was also found that the content of curcumin varies more than twofold in various commercial preparations. This illuminates the fact that the actual amount of curcumin used in various studies is often unclear (Tayyem, Heath, Al-Delaimy, & Rock, 2006). Curcumin content is infrequently measured and/or reported; this oversight waves a red flag demanding cautious interpretation of relevant literature.

Piperine is responsible for the spiciness of black pepper. Importantly, the alkaloid is an inhibitor of hepatic and intestinal glucuronidation which leads to xenobiotic metabolism. Shoba *et al* combined piperine and curcumin and examined resulting serum levels of curcumin. Interestingly, the blend of these two spices, 2g curcumin and 20mg piperine, resulted in a 154% increase in the elimination half-life and bioavailability of curcumin in rats and by a beyond belief 2000% increase in humans (Shoba, et al., 1998). Likewise, it was found that the bioavailability of curcumin was increased five-fold in both the plasma and the liver when given orally in rats the formulation of curcumin phosphatidylcholine (Marczylo et al., 2007).

1.5.2. Limited Bioavailability, Limitless Range of Targets

Intriguing is curcumin's unexpected breadth of activity far beyond the GI tract, despite the confining margins set by its poor bioavailability. In spite of these confines, it is well documented in a numerous studies that curcumin has significant biological target effects in a variety of tissues including but not limited to the brain (Lim et al., 2001), lung (Lim, et al., 2001), kidney (Farombi & Ekor, 2006), gall bladder (Rasyid & Lelo, 1999), liver (Reyes-Gordillo et al., 2007), blood (Manjunatha & Srinivasan, 2007), and immune cells (South, Exon, & Hendrix, 1997). The reason for this mysterious scope remains unknown. Possible explanations include retention of this hydrophobic molecule in biological membranes, local factors potentiating curcumin's effects and the activity of potent metabolites of curcumin (Hatcher, et al., 2008).

1.5.3. The Dangers of Curcumin

Despite curcumin's miraculous therapeutic potential, as with *all* drugs curcumin has detrimental side effects. Various studies have suggested that curcumin is both ineffective and has adverse biological effects (Hatcher, et al., 2008). For example, curcumin has shown evidence of blood thinning properties such as platelet aggregation (Hatcher, et al., 2008). Also, curcumin induced apoptotic cell death in the presence of copper and isozymes of cytochrome p450 (CYP) found in the skin, lymph, lung and liver through fragmentation of DNA and base damage (Sakano & Kawanishi, 2002; Yoshino et al., 2004). In the same way curcumin-mediated DNA damage was documented using a comet assay in lymphocytes (Urbina-Cano et al., 2006). Curcumin induced DNA-damage is not limited to in-vitro studies. In Long-Evans Cinnamon (LEC), a strain that accumulate copper in their liver, studies have shown that copper-bound curcumin loses its ability to inhibit liver and kidney tumors. Additionally, life span of the LEC rats was shortened (Frank et al., 2003). In a second study on cinnamon rats, rats were given 0.5% curcumin through food intake. It was found that Etheno-DNA adducts that play causal roles in liver cancer were increased between 9 and 25 fold in the nuclear DNA of the liver (Nair et al., 2005).

Though some studies report curcumin's beneficial induction of p53 and subsequently apoptosis (B. B. Aggarwal et al., 2007), other studies indicate an antiapoptotic effect in colon cancer cells (Sharma et al., 2004; Tsvetkov et al., 2005). Curcumin may also impede the activity of chemotherapeutic drugs. Curcumin was shown to inhibit camptothecin-induced death of breast cancer cells in culture. In the same way, curcumin weakened the cyclophosphamide-induced regression of breast tumors in nude

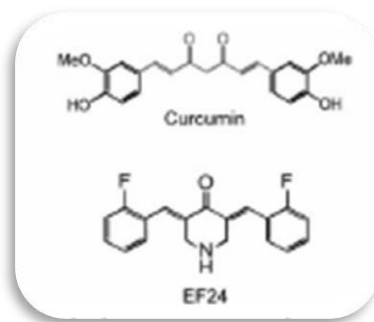
mice. However it is important to note that authors monitored tumor growth for only 3 days (Goel, Kunnumakkara, et al., 2008; Somasundaram, et al., 2002).

1.5.4. Curcumin Analogues

With the aforementioned cautionary accounts in mind, in addition to characteristics of low potency and poor bioavailability, one can see that curcumin's clinical potential remains limited (Kasinski, et al., 2008; Shoba, et al., 1998). As previously mentioned, the conundrum of curcumin's boundless target range but restricted bioavailability has brought attention to the notion that curcumin derivatives or metabolites have enhanced biological properties. In fact metabolites like tetrahydroxy curcumin have been found to possess anti-inflammatory and anti-oxidant properties similar to their parent compound curcumin (S. Singh & Khar, 2006).

What's more, curcumin has emerged as the perfect lead compound for further chemical modifications and optimizations (Adams et al., 2005; Adams et al., 2004) as well as for the design of novel chemotherapeutic agents (Hatcher, et al., 2008).

In 2004 Adams et al aimed to synthesize such novel curcumin analogues with anti-cancer activity. Prior to the synthesis of novel compounds, data base searches were performed to identify commercially available, potentially biologically active monoketone analogues. Two compounds emerged and were tested in in-vitro cell viability screens. It was found that the two monoketone containing molecules were more active than curcumin. In a further study a number of such molecules were synthesized and biologically evaluated.



(Kasinski, et al., 2008)

To produce monoketones, two carbons and an oxygen were removed from the center of the molecule, a heterocyclic ring including the newly created ketone was affixed and terminal ring substituents were varied. Ten analogues were weeded out from a pool of 100, and were later evaluated in National Cancer Institute's 60 panel of cell lines. EF24 or 3,5-Bis(2-fluorobenzylidene)piperidin-4-one, with its simple and symmetrical structure, came forward as one of the best candidate compounds (Adams, et al., 2004; Kasinski, et al., 2008).

1.5.5. The Novel Curcumin Analogue EF24 and Its Anti-Cancer Potential

Characterized by potent biological effects and distinct chemical properties, EF24 represents a novel class of redox-dependent anti-cancer agents (Adams, et al., 2005). Via a mechanism dependent on ROS production, caspase-3 activation, phosphatidylserine externalization and DNA fragmentation, EF24 induces G2/M arrest and apoptosis in MDA-MB 231 human breast cancer and DU-145 human prostate cancer cell. A lower dose of EF24 than that of curcumin has also been shown to inhibit growth of human breast tumors in a mouse xenograph, notably with a retained safety profile (Adams, et al.,

2005; Adams, et al., 2004; Kasinski, et al., 2008). EF24 additionally disrupts mitochondrial function, evident by the depolarization of mitochondrial membrane potential. In wild-type and Bcl-xL overexpressing HT29 cancer cells, EF24 has been shown to reduce intracellular GSH and GSSG. Similar to curcumin, EF24 reacts with glutathione (GSH) and thioredoxin 1 serving as a Michael acceptor reacting. Data suggests that EF24 may also have a multi-targeted approach as it relates to mediators containing SH groups (Adams, et al., 2005; Dinkova-Kostova, Massiah, Bozak, Hicks, & Talalay, 2001).

1.5.6. EF24 vs. Curcumin: A Brief Comparison

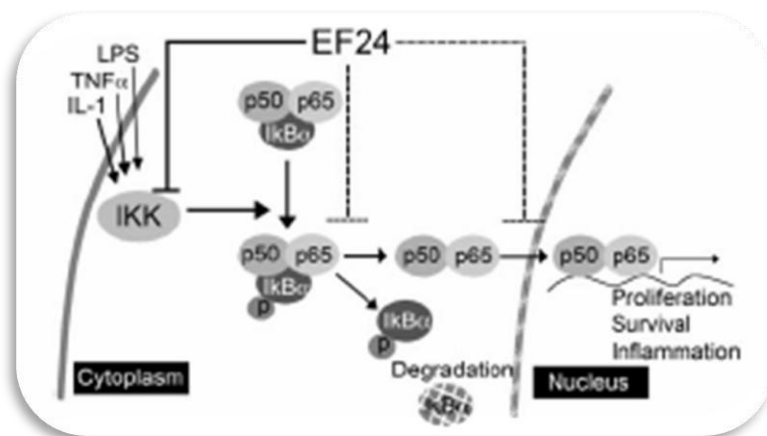
In comparison to curcumin, EF24 has been shown to induce apoptosis through cell cycle arrest in a number of cell lines with a much higher potency. It was reported that the IC_{50} of EF24 is 10 (prostate cell line) to 20 (for all other cell lines) times lower than that of curcumin in non-small cell lung, ovarian, cervical, breast and prostate cancer cells (Kasinski, et al., 2008). A sulforhodamine B assay was performed to determine cell viability. It was reported that the IC_{50} value for curcumin ranged from 15 to 20 μ M and 0.7 to 1.3 μ M for EF24. These findings corroborate the enhanced cytotoxic activity of EF24 over curcumin.

1.5.7. EF24 Suppresses the NF- κ B Pathway through I κ B Kinase

Even though NF- κ B is a crucial target of curcumin, a direct inhibitory effect on IKK β has not been shown. Kasinski *et al* have identified EF24 as a new class of IKK β

inhibitors (Kasinski, et al., 2008) and a lead compound for novel, more potent IKK β inhibitors (Karin, 2006a).

Unlike the aforementioned canonical or non-canonical pathway, the working model of NF- κ B related to the mechanism of EF24 signaling involves subunits p50, p65 and I κ B α .



(Kasinski, et al., 2008)

Using high content analysis, it was found that EF24 rapidly blocks NF- κ B nuclear translocation. Additionally it was determined from western blot analysis that EF24 inhibits the phosphorylation and degradation of IKK induced by TNF- α . Lastly it was found that the catalytic activity of IKK was directly inhibited by EF24 in an in-vitro reconstituted system. EF24's direct targeting of IKK begins to elucidate its enhanced efficacy in comparison to curcumin (Kasinski, et al., 2008).

1.6. “Starting from Scratch, Ending with Stoppers: A Discussion of Various Technologies to Measure Migration In-Vitro”

1.6.1. Migration as an Essential Step of Metastasis

Tumor cell mobilization is the first step in the complex process of metastasis. Migration in itself is just as complex, and is implicated in several biological events including wound healing, angiogenesis, tissue formation and immune responses. Migration is characterized by several molecular changes such as the reorganization of actin filaments and microtubules, polarization of the secretory apparatus, membrane protrusion, and dynamic adhesion to the substrate. Such mobilization is usually triggered by an extracellular signal which then activates a signal transduction cascade (Soderholm & Heald, 2005; Yarrow, Perlman, Westwood, & Mitchison, 2004).

1.6.2. Cell Migration Assays

There are four major classes of cell migration assays. The first is the transmigration assay which evaluates migration of cells based on their ability to traverse the vascular endothelium. For example CytoSelect™ engineers Transmigration Assays in which the inserts are coated with endothelial cells. Second is the haptotaxis assay, which gauges migration in a gradient of chemoattractants. CytoSelect™ Cell Haptotaxis Assays employ the traditional Boyden chamber; the underside of the membrane inserts are coated with Collagen I or Fibronectin. Third is the chemotaxis assay which measures migration based on a chemical environment. CytoSelect™ also markets a chemotaxis assay that mimics the set up of the haptotaxis assay but lacks the coated membrane inserts. These

assays are available in low throughput (24-well) and high-throughput (96-well) format (Shaffer, 2009).

1.6.3. The Wound Healing Assay: “Starting From Scratch”

Fittingly, the theory which defines tumors as “wound that never heals” is the essence of the final and most relevant type of cell migrations assay. When a wound or scratch is introduced to a monolayer of cells, wound healing is induced by growth factors and disruption of cell-cell contacts at the margin of the wound. Recovery of the monolayer is executed by both proliferation and migration of cells to fill in the gap (Coomber & Gotlieb, 1990; Falzano et al., 1993; Yarrow, et al., 2004; Zahm et al., 1997).

To perform a wound healing a scratch or similar wound is made in a monolayer of cells using an object such as a pipette or syringe needle in a low throughput or high-throughput format. Wound healing is subsequently observed over a period of 3 – 72 hours. The progression of the wound healing process can be observed by fixing and manually imaging samples in an end-point assay or by a kinetic assay utilizing time-lapse microscopy (Yarrow, et al., 2004). Wound healing assays can be applied to thorough studies of cell biology, to investigate the effects of perturbations on migration, and most central to this work – to the discovery and validation of small molecule leads (Mc Henry, Ankala, Ghosh, & Fenteany, 2002).

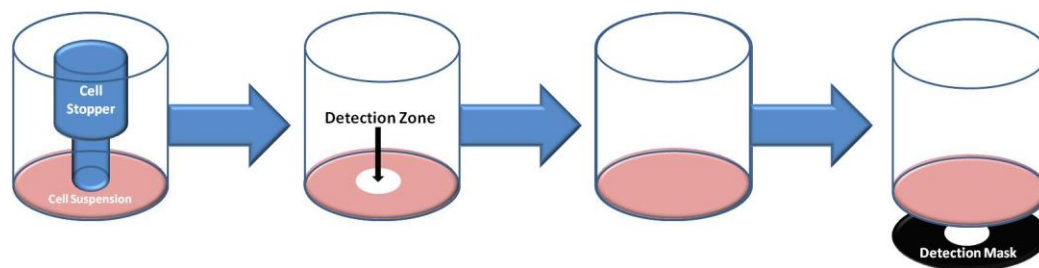
The traditional wound healing assay measures the time required for the monolayer to recover and close a scratch. However, this assay is preceded by its reputation of inconsistency due to variation in scratch size. Additionally cells at the wound margin may suffer damage upon wounding which jeopardize healthy migration of the cells. On the

contrary, CytoSelect™ offers a wound healing assay. This assay offers the several advantages over the conventional wound healing assay including the creation of a uniform and consistent 0.9mm gap across the diameter of the well with precise plastic inserts and no damage inflicted upon the marginalized cells. Cells are subsequently seeded and create a monolayer around the gap (Shaffer, 2009).

1.6.4. The Platypus Cell Migration Assay: “Ending with Stoppers”

Though the CytoSelect™ Wound Healing Assay offers several benefits over conventional assays, it is available only in 24-well low throughput format (Shaffer, 2009). For the purpose of this study, the necessary application of the wound healing assay is to the discovery and validation of small molecule leads. Consequently the wound healing assay for this study must be available in high-throughput format. Recently, a few key innovations in high-throughput format have emerged. For example, Yarrow et al. has adapted the scratch wound healing assay to 384-well format. Monolayers were mechanically scratched with a pin array, and regularly sized wounds were created in all wells.

Another significant innovation is manufactured by Platypus Technologies. The Oris™ cell migration assay is uniquely designed to generate more reproducible results than conventional assays, and is less bulky than Boyden chamber devices. The Oris™ assay uses medical grade silicon inserts referred to as “cell stoppers” in a 96-well plate. The assay is available in three coatings including tissue-culture-, Collagen I- and Fibronectin-coated plates.



("Oris™ Cell Migration Assay," 2010)

Stoppers are inserted into each well and seal off a 2mm circular region. Cells are seeded into ports on either side of the silicone cell stopper. Cells form a uniform monolayer around the periphery of the stopper. Upon removal of the stopper with a special multipronged tool called the “stopper tool”, a region in which no cells were seeded is created. Cells are allowed to migrate into this circular 2mm “detection zone.” Results can be collected by affixing the “detection mask” or “plate mask” to the plate and using various instruments including a microscope, digital imaging system or fluorescence plate reader.

The features and benefits of the cell migration assay boasted on the Platypus website include:

- Membrane-free migration - no cumbersome cell culture inserts; stain and view cells in the same well.**
 - **Reproducible results - the unique design provides well-to-well CV's < 12%.**
 - **Preserve cell morphology - changes in cell structure can be monitored in real time**
 - **Versatile - analyze data using multiple probes in a single well using a microscope, digital imager, or fluorescence plate reader.**
- Flexible - design kinetic or endpoint based cell migration assays without the use of special instrumentation.** ("Oris™ Cell Migration Assay," 2010)

The Oris™ cell migration assay will be utilized in this study with A549 lung cancer cell line.

1. 7. Experimental Purpose

The purpose of this study was to examine the effect of novel curcumin analogues on the metastatic potential of cancer cells using a high-throughput image-based cell migration assay in a 96-well format. The high-throughput cell migration assay was developed by Platypus Technologies. The unique migration assay was utilized in conjunction with the ImageXpress5000 automated fluorescent microscope. The feasibility of the Oris™ Cell Migration Assay for the high-content screen was assessed and the imaging protocol and data analysis methods were optimized. 3,5-Bis(2-flourobenzylidene)piperidin-4-one (EF-24) and related analogs of curcumin were tested to assess their effect on the migratory potential of cancer cells and ranked based on their potent inhibitory capabilities. The effective inhibition of the migratory potential of cancer cells may lead to the development of a new generation of novel antimetastatic drugs.

CHAPTER 2: Materials and Methods

2.1. Materials

Curcumin was purchased from Alfa Aesar (Ward Hill, MA), and its structural analog, EF24, was prepared as reported previously (Adams et al., 2004). AM5, AM10 and AM12 are novel analogues prepared by Xuesong Yang. All compounds were dissolved in DMSO, with a stock concentration of 10mM or 5 mM. TNF- α Sigma-Aldrich (St. Louis, MO) was resuspended in water to a final concentration of 10 μ g/ml. Cells were stained with Hoechst 33258, 98% form Across Organic, and fixed with Para-formaldehyde Sigma-Aldrich (St. Louis, MO)

2.2. Cell Cultures

Cells were maintained Dulbecco's modified Eagle's medium (A549), with 10% fetal bovine serum and penicillin/streptomycin in a 37°C incubator with 5% CO₂.

2.3. Cell Migration Assays

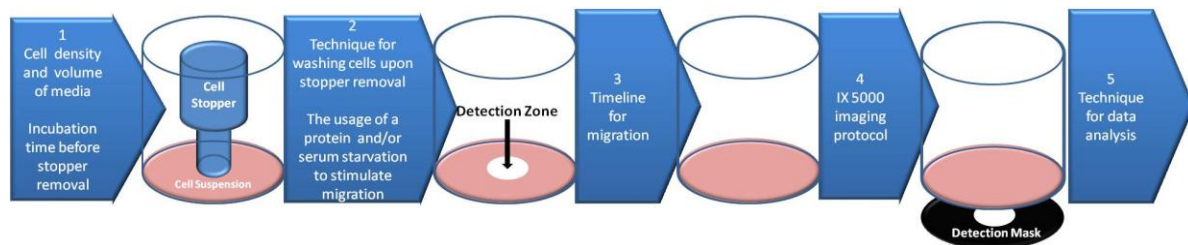
A549 cells (in media containing 10% FBS) were seeded into Oris™ 96-well plates at 40,000 cells/well and allowed to grow overnight. After stopper removal, cells were washed with PBS and media was replenished. Cells were treated with compounds for 4 h before addition of TNF- α (10 ng/mL). Cells were then allowed to migrate for 72 hours and then fixed in 2% para-formaldehyde and stained with Hoechst 3258. Imaging was performed using the Image Express 5000 from Molecular Devices. Images were analyzed using ImageXpress Software and ImageJ Freeware (NIH).

CHAPTER 3: Results

3.1. Assay Development for Experimental Conditions

Assay development was an integral part of this study. To assess the ability of curcumin and its analogues to inhibit migration each step in the Oris™ cell migration assay protocol had to be carefully optimized.

Figure 1 is the visualization of a seeded well in the Oris™ cell migration assay without (Image A) or with (Image B) the plate mask (detection mask according to the Oris™ cell migration assay protocol). Indicated on the images are the different regions of images as they appear in the work. Also, colored arrows label the names of the regions as they will be referred to in this work. The plate mask is an opaque attachment that is affixed to the bottom of the 96-well plate as depicted in Image C. It contains 96 circular apertures that align with the detection zone of each well (Image C).



Redrawn from ("Oris™ Cell Migration Assay," 2010)

As outlined in materials and methods the migration assay consists seeding cells into the Oris™ 96-well plates, incubation for growth, stopper removal, a PBS wash, replenishment with fresh media, compound treatment and or stimulation, incubation for

migration, imaging and lastly data analysis. Upon the completion of the assay the Oris™ 96-well plate was imaged and analyzed.

First, the optimal seeding density and volume of media for the cell suspension was determined as represented by step 1 of the schematic above. Figure 2 is a visualization of the various densities of cells and volumes of media attempted in the assay. In Image A, A549 cells were suspended at a density of 40,000 cells per well and 50µL of media per well. These conditions resulted in the uneven distribution of cells around the detection zone. In Image B, the cell density was increased to 50,000 cells per well and the volume of media was increased to 100µL. These conditions resulted in even seeding. Lastly, 100,000 cells per well in 100 µL of media were seeded. This resulted the peeling away of the monolayer of cells from the collagen coated surface of the plate. The incubation time for growth was dependent upon the density of cells seeded.

Next, the precise method for washing the cells, and more generally the techniques for addition and removal of reagents required optimization as represented in step 2 of the schematic. Figure 3 depicts a vertical scratch from a pipette tip which disrupted the detection zone.

Step 3 of the schematic involves determining the timeline for migration. In all experiments incubation time allotted was 72 hours.

Screenshots of the optimized settings of the IX5000 are depicted in Figures 4, 5 and 6. This step in assay development is represented by step 4 of the schematic. Figure 4 is a visualization of the customized settings for the Oris™ cell migration assay 96-well plate: <number of rows> = 8, <number of columns> = 12, <well shape> = circle, <well diameter> = 6500, <column spacing> = 9000, <plate length> = 127.8, <column offset> =

14400, <row spacing> = 9000, <plate width> = 85.5, <row offset> = 11200, <well depth> = 12000, <plate height> = 14.9, <optical thickness> = 250 and <bottom variation> = 120.

In the <Objective and Camera> tab, <magnification> and <camera binning> settings were configured as depicted in Image A, Figure 5. In the <Wells to Visit> tab, all wells were selected and <visit multiple sites per well> was not checked as shown in Image B. <Timelapse> was set to 1 timepoint, and <Fluidics> remained on default settings (not pictured). In <Acquisition Loop>, <number of wavelengths> was set to 1 and <Enable laser-based focusing> was checked as shown in Image C.

In <Autofocus>, the <Skip Find Sample> option was selected as shown in Figure 6, Image D. Under <W1>, <Illumination setting> was set to DAPI, <Exposure> set determined by using the <AutoExpose> button, <Target maximum intensity> to 3,000 and <Autofocus options> were set to laser with z-offset with post-laser offset at 0. Finally the remaining tabs <Journal>, <Display Settings> and <Post Acquisition> remained at default settings.

Figure 7 depicts a schematic displaying the steps to the analysis of IX5000 images using MetaXpress software threshold analysis (“the Manual MetaXpress Technique”). Images could be analyzed either without (shown in the left column) or with (shown in the right column) the plate mask affixed to the Oris™ Cell Migration Assay 96-well plate.

Without the plate mask, a circular region of interest (indicated by the pink arrow and dotted circular outline) was created using reference wells (“T0”) as depicted by Image A. Reference wells are wells in which stoppers remain in place for the entire

duration of the experiment. These wells serve as a control in which migration is prohibited.

With the plate mask intact, a region of interest was created instead by using the outline of the circular aperture in the mask as shown in Image B in the right column. The threshold was set for light objects in Image B in both the left and right columns, making sure to use the same values for all images in a single plate by utilizing the <Set> option while thresholding. Subsequently, the area covered by the threshold was recorded as depicted in Image C. “Rogue cells” in the center of the matrix were excluded from the analysis if present, as show in Image D.

A flowchart depicting an alternative method for IX5000 image analysis is visualized in Figure 8. Images with the plate masks intact were analyzed using Image J software (the Platypus ImageJ Technique). After the region of interest was created using the circular aperture of the plate mask, images were thresholded using the same threshold values for each image in a single plate by utilizing the <Set> option. The <Analyze Particles> function was subsequently run ensuring the options <Show Masks>, <Summary> and <Exclude on Edges> were selected. Also the minimum and maximum <Particle Size> was defined as 100 and 1000 pixels², respectively. Similarly,<Circularity> was defined as 0.00-1.00. The analysis correcting for rogue cells can be applied to Image J analysis as well.

Figure 9 illustrates a second method of analysis using ImageJ software (the “Custom ImageJ Analysis Technique).

Image analysis as depicted in Image A was performed using the Macros depicted in Image B. The macros contained the following commands with the line breaks and indicated:

```
run("Find Edges");  
run("Enhance Contrast", "saturated=7");  
  
run("Make Binary");  
run("Watershed");  
//setTool(1);  
makeOval(462, 338, 356, 374);  
makeOval(421, 338, 397, 383);  
makeOval(421, 300, 397, 421);  
makeOval(421, 300, 411, 421);  
makeOval(391, 300, 465, 446);  
  
run("Analyze Particles...", "size=10-Infinity circularity=0.00-1.00  
  
show=Masks  
  
exclude summarize");
```

Image C shows the analysis correcting for rogue cells using this customized technique.

3.2. Data Analysis and Data Collected

Initial trials of the Oris™ cell migration assay were run to determine the effects of curcumin and EF24 on A549 cell migration. Images were analyzed using MetaXpress software with threshold area percent as the readout. In Figure 10, curcumin dosage ranged from 20µM at the highest to 2.5µM at the lowest. Standard deviations were larger at higher concentrations and overall there was a slight but not statistically significant decreasing trend in threshold area percent with increasing concentration. There was no change in threshold area percentage of drug treated wells in comparison to the control

(DMSO) condition. Also no change was evident in threshold area percent with increasing curcumin concentration.

EF24 dosage ranged from 1 μ M at the highest to 0.125 μ M at the lowest in Figure 11. The standard deviations are minimal at all concentrations and overall the line of best fit had a slope close to 0. There was no change in threshold area percentage of drug treated wells in comparison to the control (DMSO) condition. No change was evident in threshold area percent with increasing curcumin concentration.

Figure 12 and 13 compare the reference wells, to the control wells, to the highest concentration of curcumin or EF24 used. 20 μ M curcumin exhibited a statistically significant decrease in comparison to DMSO as shown in Figure 12. However, 1 μ M EF24 showed no change in comparison to DMSO as shown in Figure 13.

Data analysis for Figures 10-13 were performed using the “Manual MetaXpress Analysis Technique.”

Figures 14-16 show the effect of increasing the dosage of EF24, AM12 and AM5 respectively. A linear decrease in migrated cell count with increasing concentrations was not observed for any of the corresponding drug conditions.

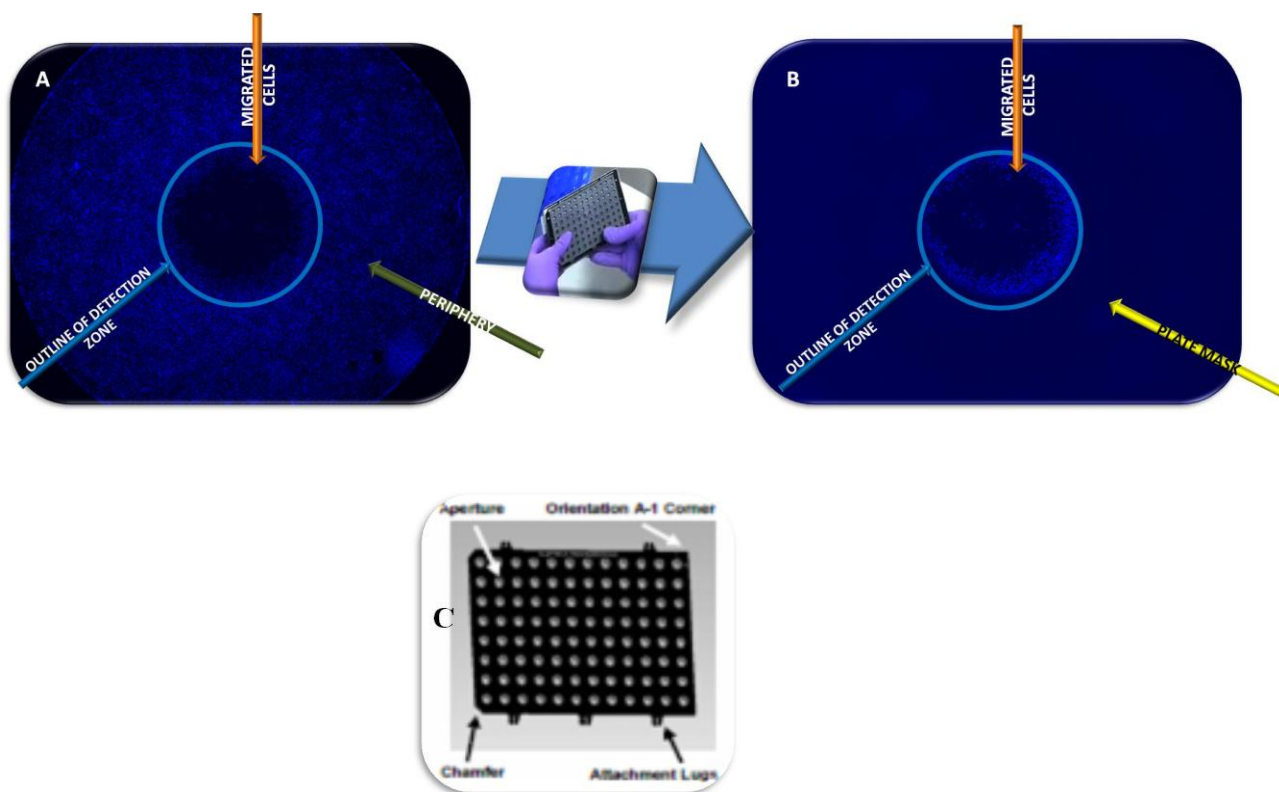
Figures 17 and 18 show the effect of increasing the dosage of curcumin and AM10 respectively. A linear decrease in migrated cell count with increasing concentrations was evident in both drug conditions.

Lastly, Figure 19 depicts the most effective concentration of each drug in comparison to the two control wells. There was a statistically significant increase in DMSO in comparison to DMSO+ TNF- α . In addition all drug treated wells induced a

statistically significant decrease in the number of cells that migrated into the detection zone.

Data analysis for figures 14-19 were performed using the “Custom ImageJ Analysis Technique.”

3.3. Figures



("Oris™ Cell Migration Assay," 2010)

Figure 1 Labeled image of wells, without **A**; and with the plate mask **B**. The plate mask is depicted in **C**.

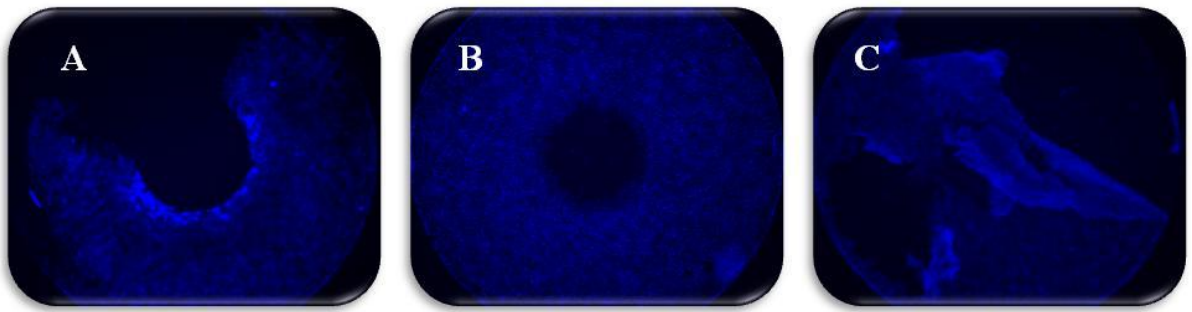


Figure 2 A549 cells seeded at 40,000 cells per well, and 50 μ L of media **A**; 50,000 cells per well and 100 μ L of media **B**; 100,000 cells/well and 100 μ L of media **C**.

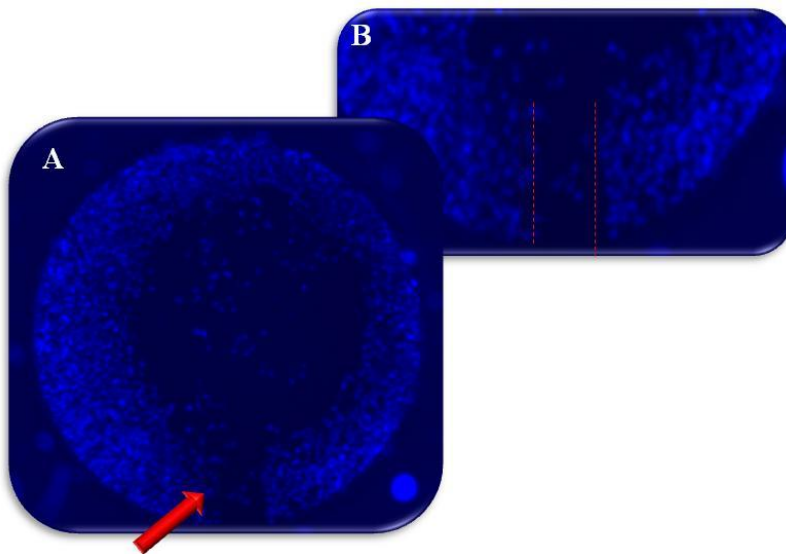


Figure 3 Monolayer of A549 cells seeded at 50,000 cells per well disrupted by a pipette tip scratch **A**; an enlargement of the scratch **B**.

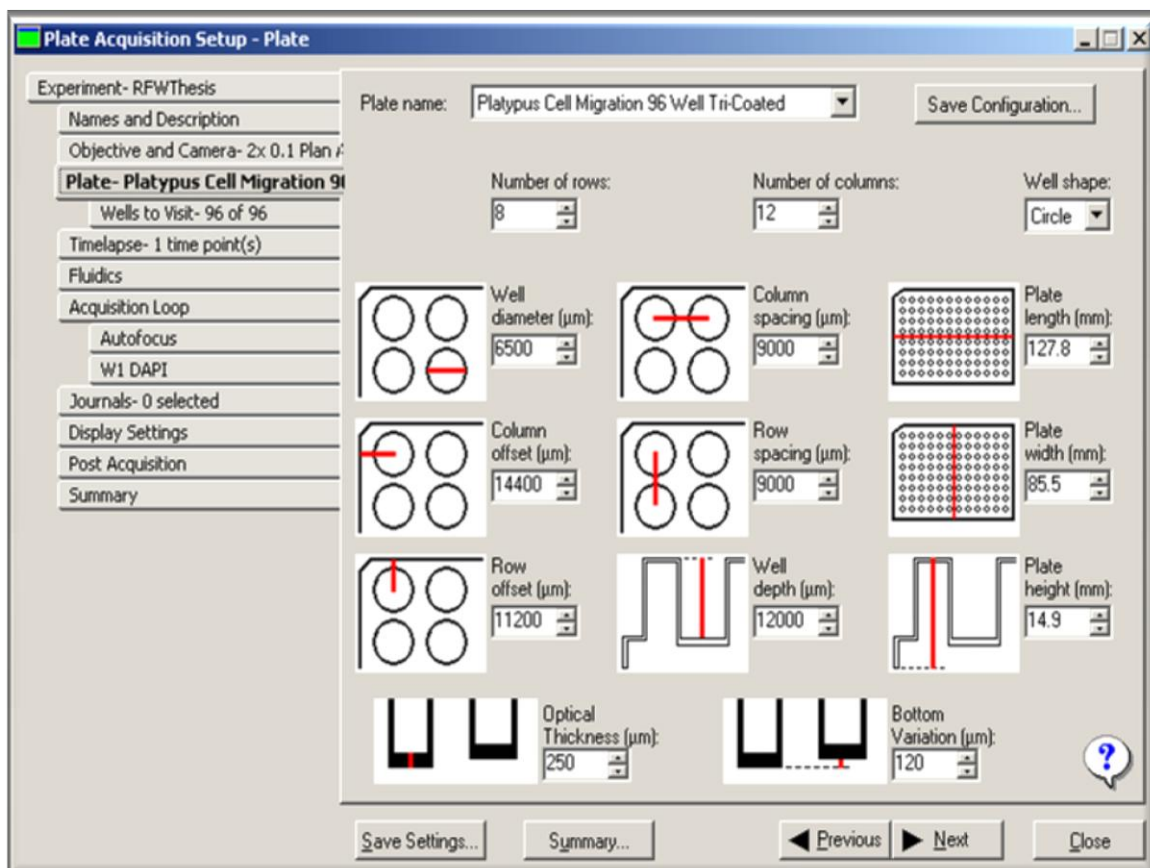


Figure 4 Screenshot of the settings for the IX5000 displaying customized settings for the Oris™ cell migration assay 96 well plate.

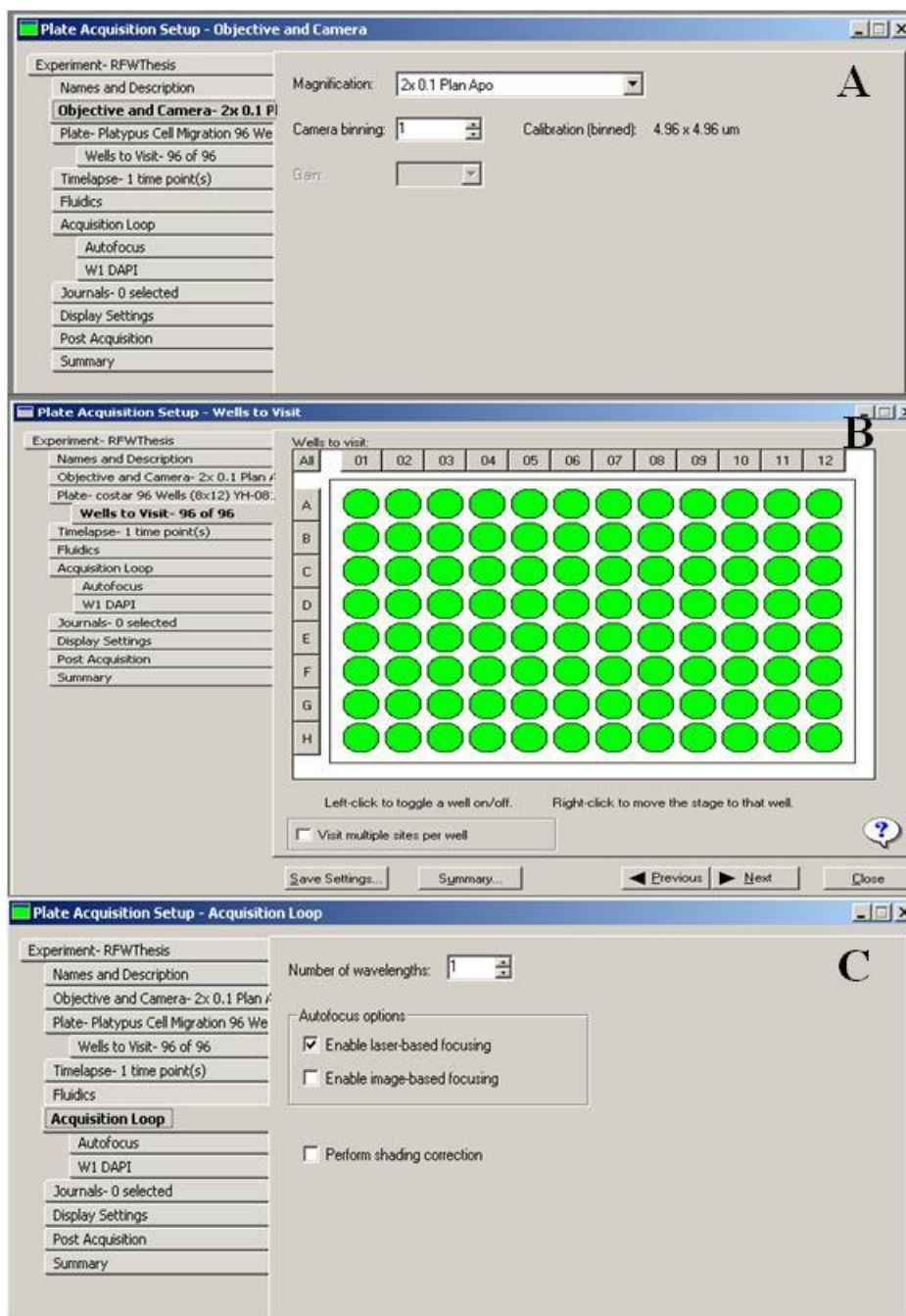


Figure 5 Screenshot of the settings for the IX5000 displaying customized settings for the Objective and Camera **A**; Wells to Visit **B** and Acquisition Loop **C**.

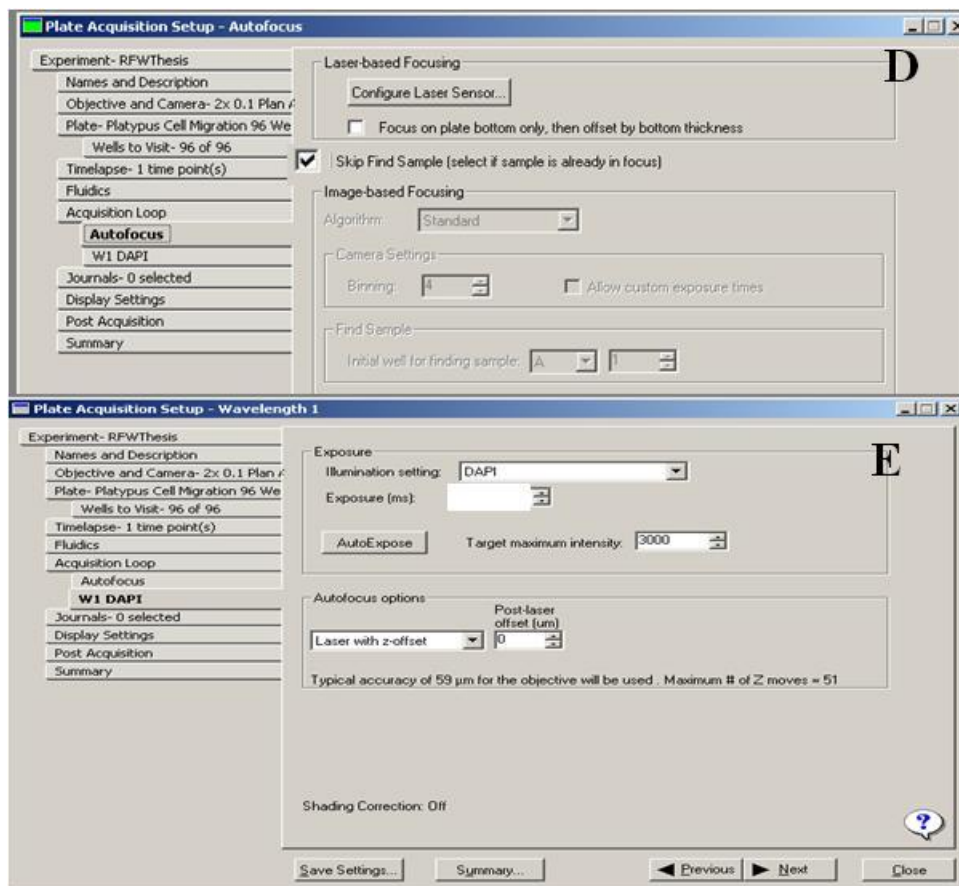


Figure 6 Screenshot of the settings for the IX5000 displaying customized parameters for the Autofocus **D** and Wavelength 1 **E**.

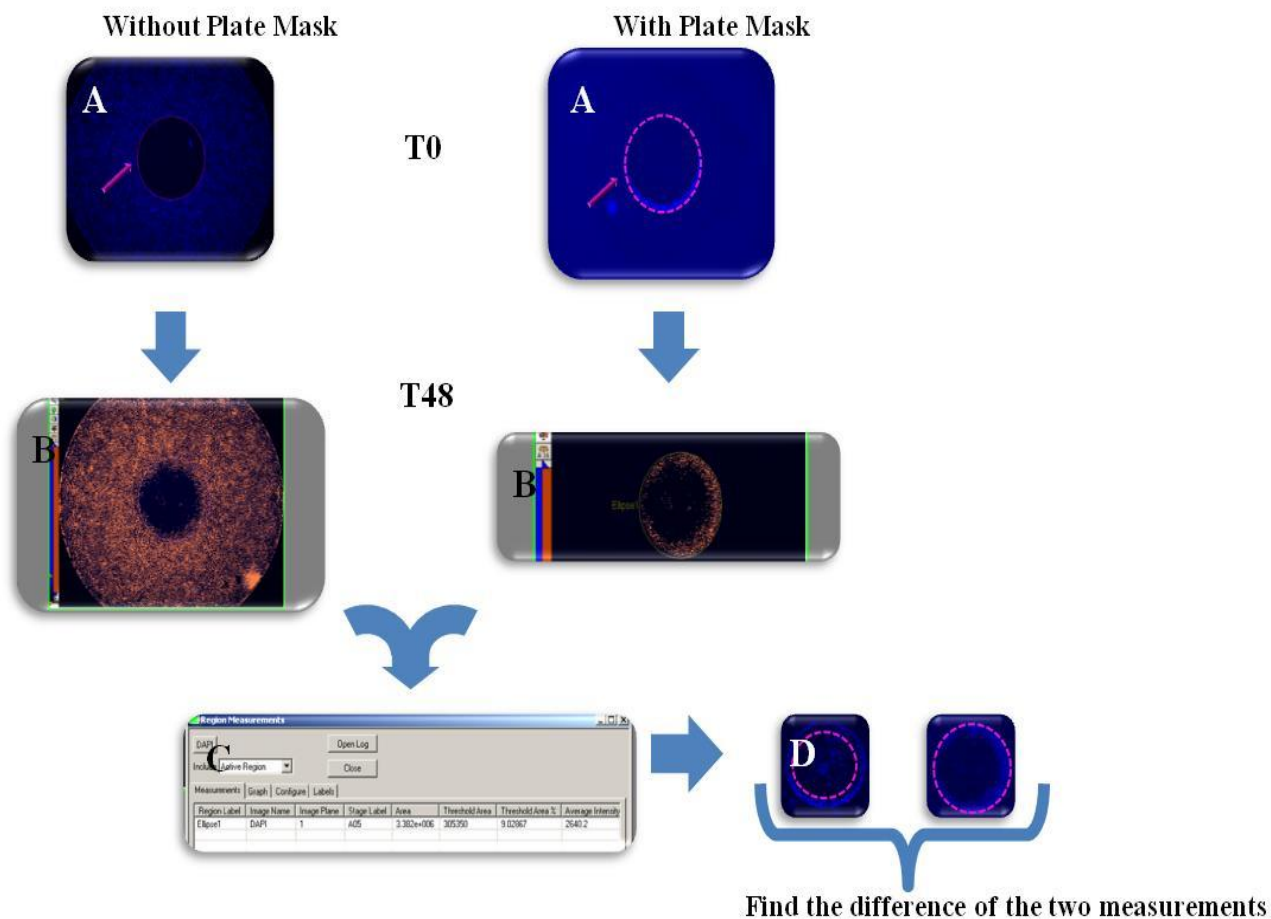


Figure 7 “MetaXpress Manual Technique.” A flow chart depicting the analysis of IX5000 images using MetaXpress software. Timepoint 0 is visualized in **A**; images labeled **B** have been analyzed at the 72 hour timepoint; **C** depicts the subsequent recording of data; **D** represents further analysis of images to correct for “rogue cells”.

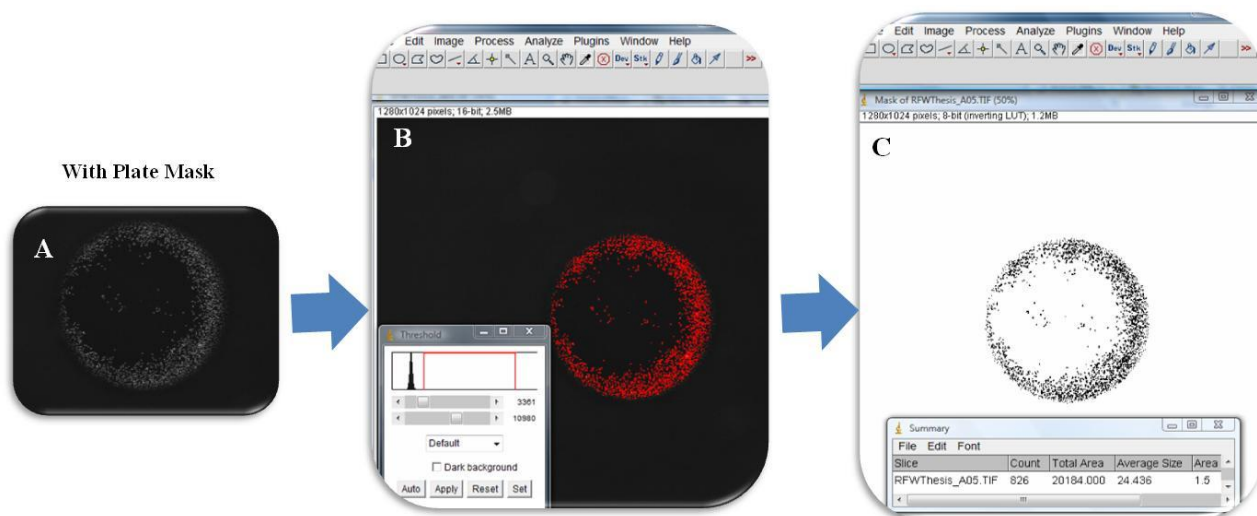


Figure 8 “Platypus ImageJ Technique.” A flow chart depicting the analysis of IX5000 images using Image J software. Images were analyzed with the plate mask affixed to the Oris™ Cell Migration Assay 96-well plate. A circular region of interest was created using the aperture of the plate mask **A**; a threshold was set for light objects **B**; particles were then analyzed **C**.

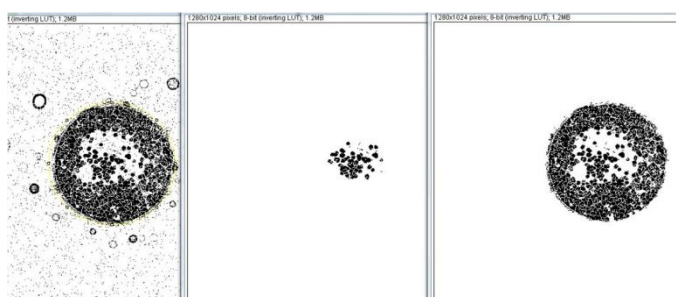
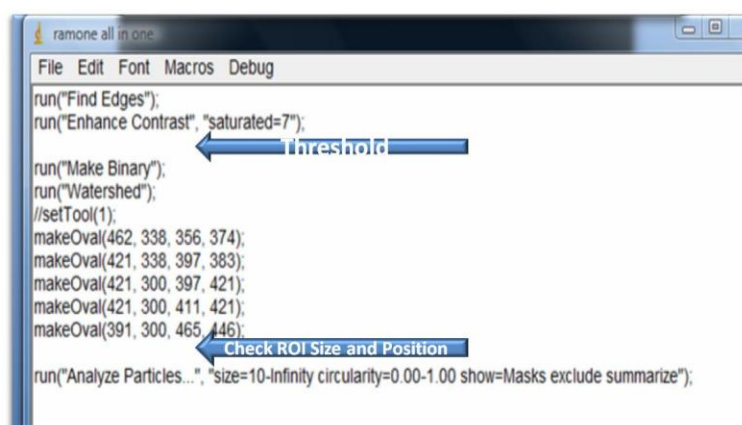
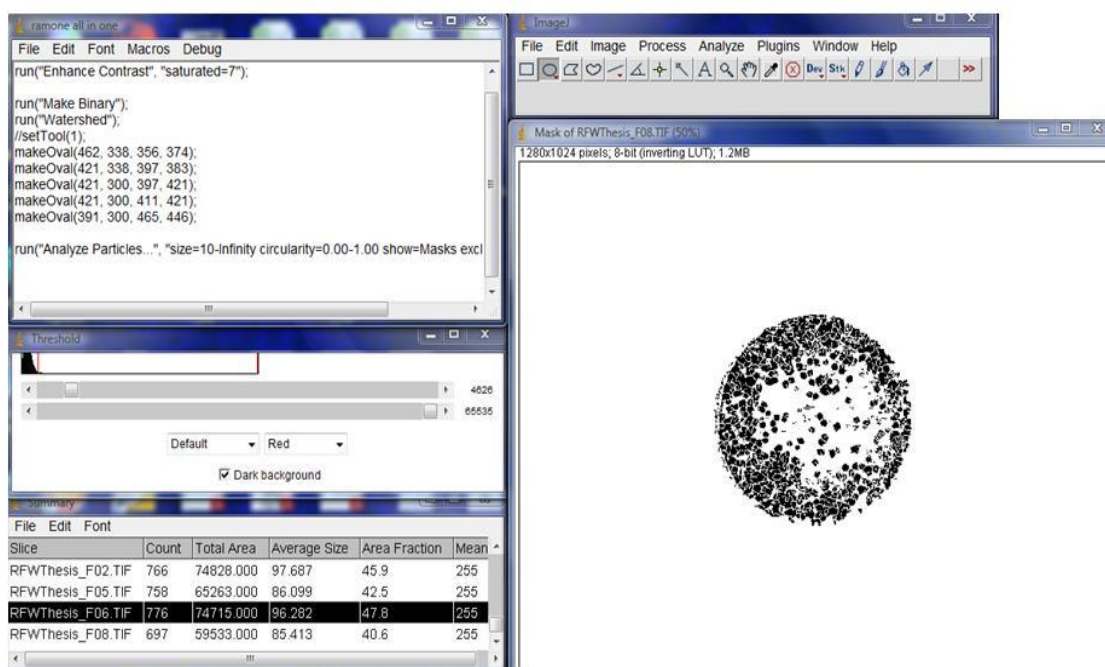


Figure 9 “Custom ImageJ Technique.” Screenshots depicting the analysis of IX5000 images using Image J software. Images were analyzed with the plate mask affixed to the Oris™ Cell Migration Assay 96-well plate. A the steps (A) of a custom Macros (B) were executed. Analysis of “rogue cells” was performed as well C.

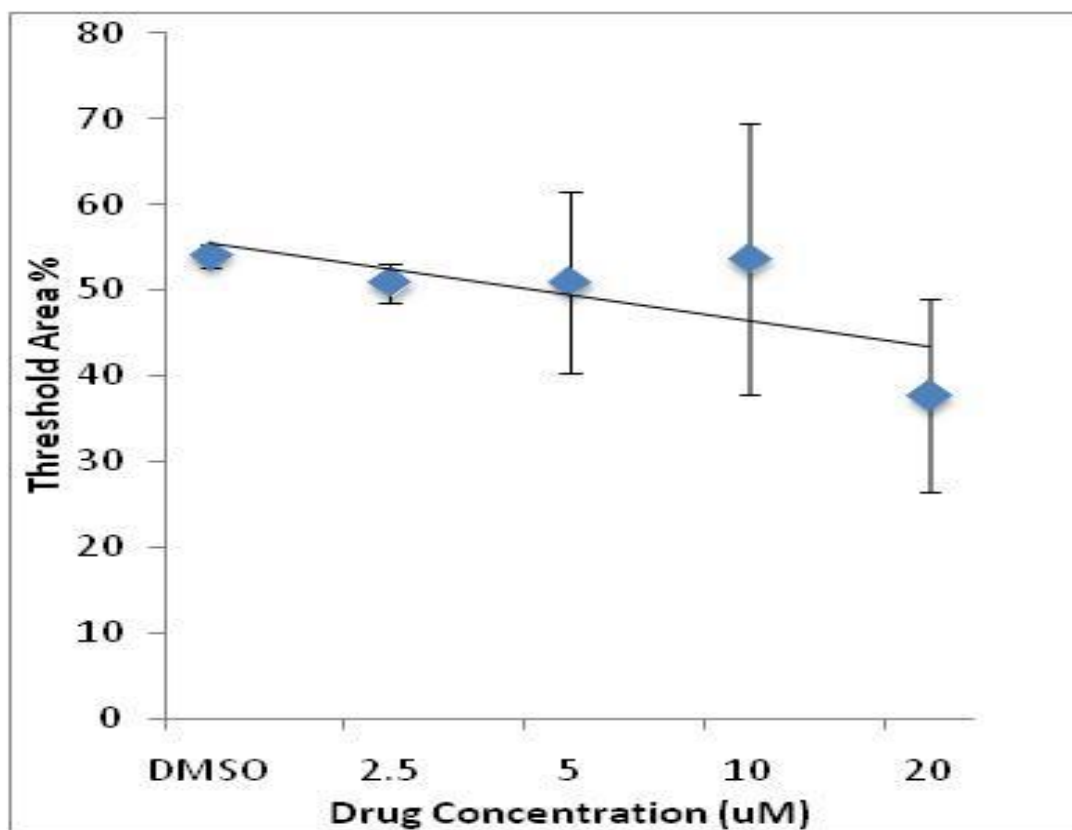


Figure 10 A549 cells were treated with increasing doses of curcumin and percentage of area covered by migrated cells was determined after 72 hours. Data was analyzed using the “MetaXpress Manual Technique.”

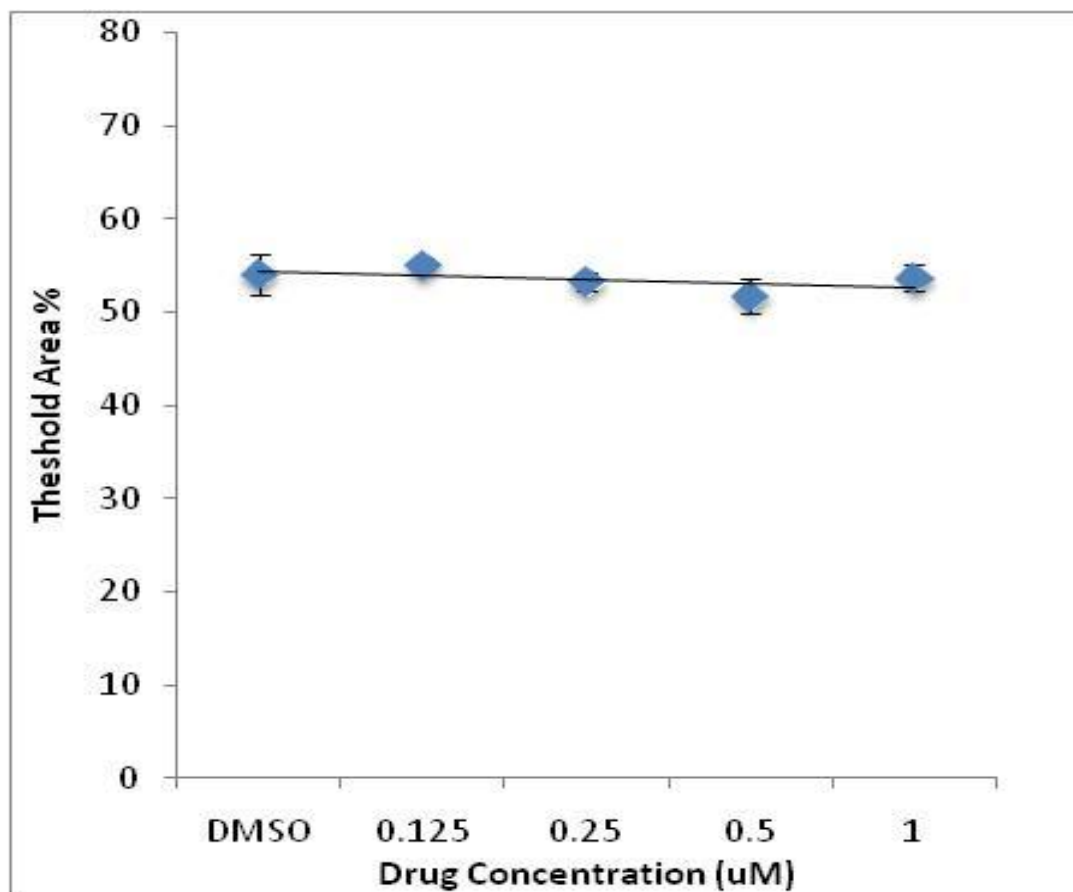


Figure 11 A549 cells were treated with increasing doses of EF24 and percentage of area covered by migrated cells was determined after 72 hours. Data was analyzed using the “MetaXpress Manual Technique.”

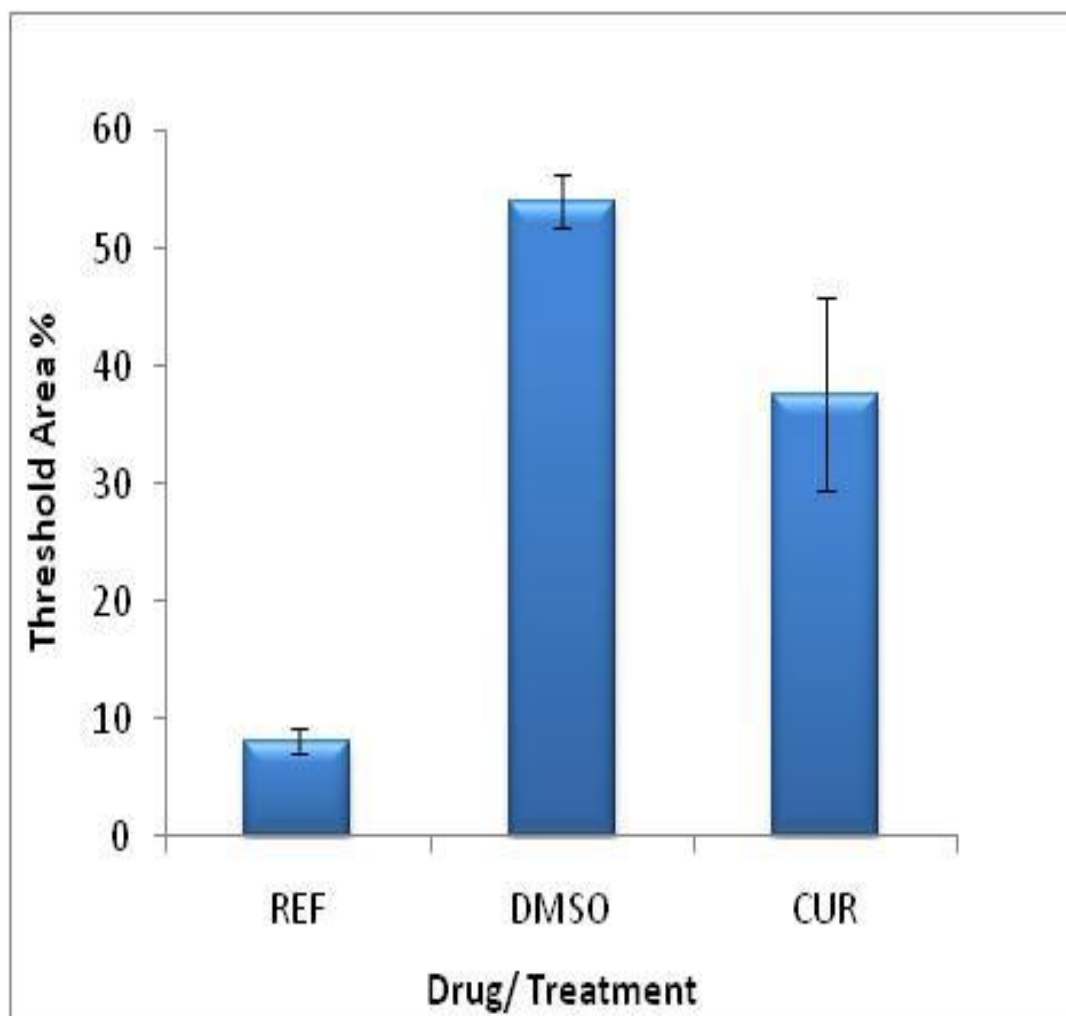


Figure 12 A comparison of “Reference” wells to control wells or “DMSO” to 20 μ M curcumin after 72 hours of migration. The y-axis indicates the percentage of the total area of the detection zone covered by migrated cells. Data was analyzed using the “MetaXpress Manual Technique.”

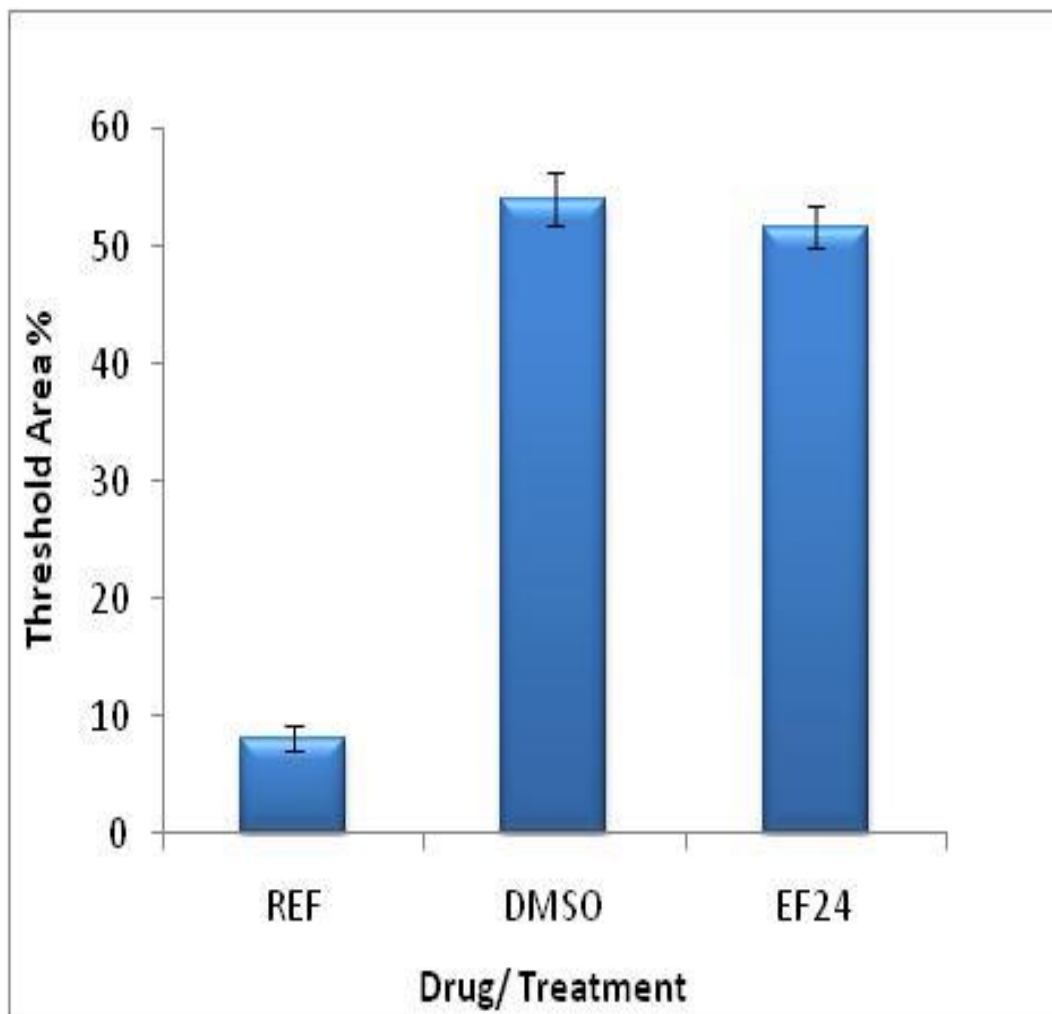


Figure 13 A comparison of “Reference” wells to control wells or “DMSO” to 1 μ M EF24 after 72 hours of migration. The y-axis indicates the percentage of the total area of the detection zone covered by migrated cells. Data was analyzed using the “MetaXpress Manual Technique.”

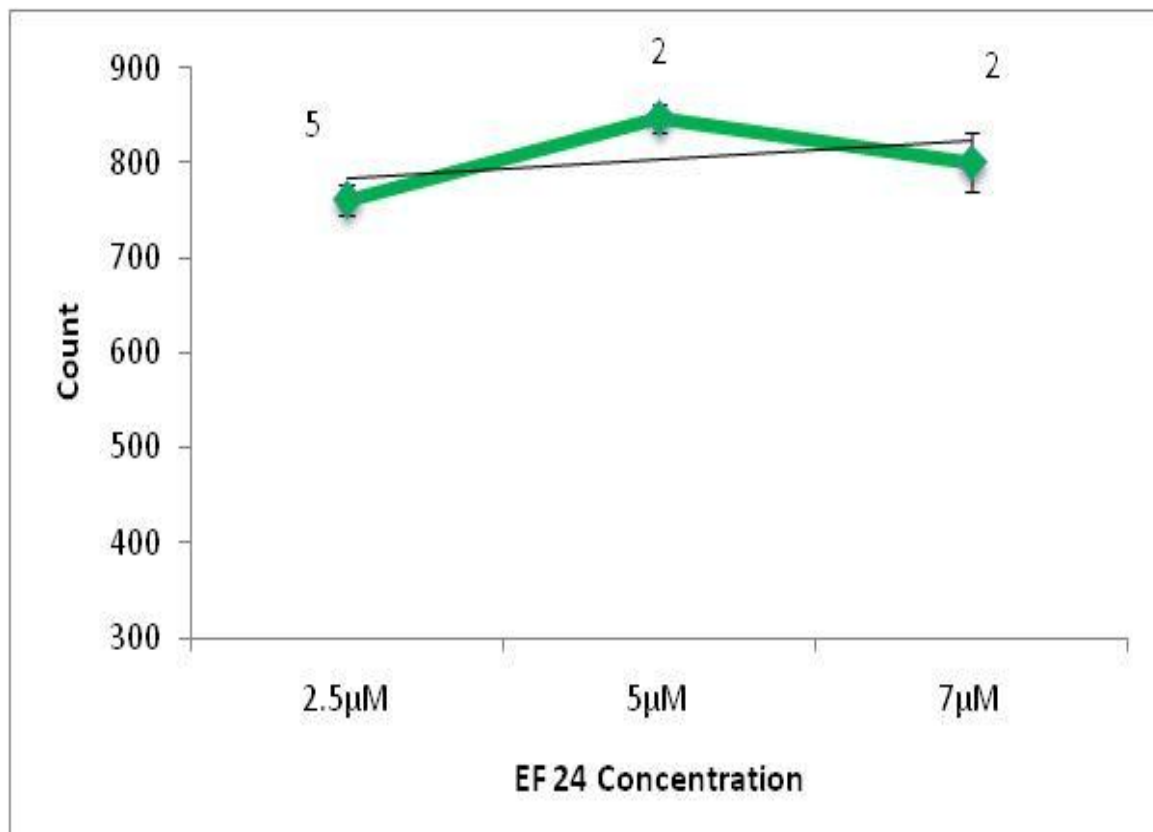


Figure 14 A549 cells were treated with increasing doses of EF24 and percentage of area covered by migrated cells was determined after 72 hours. Data was quantified using the “Custom Image J Technique.”

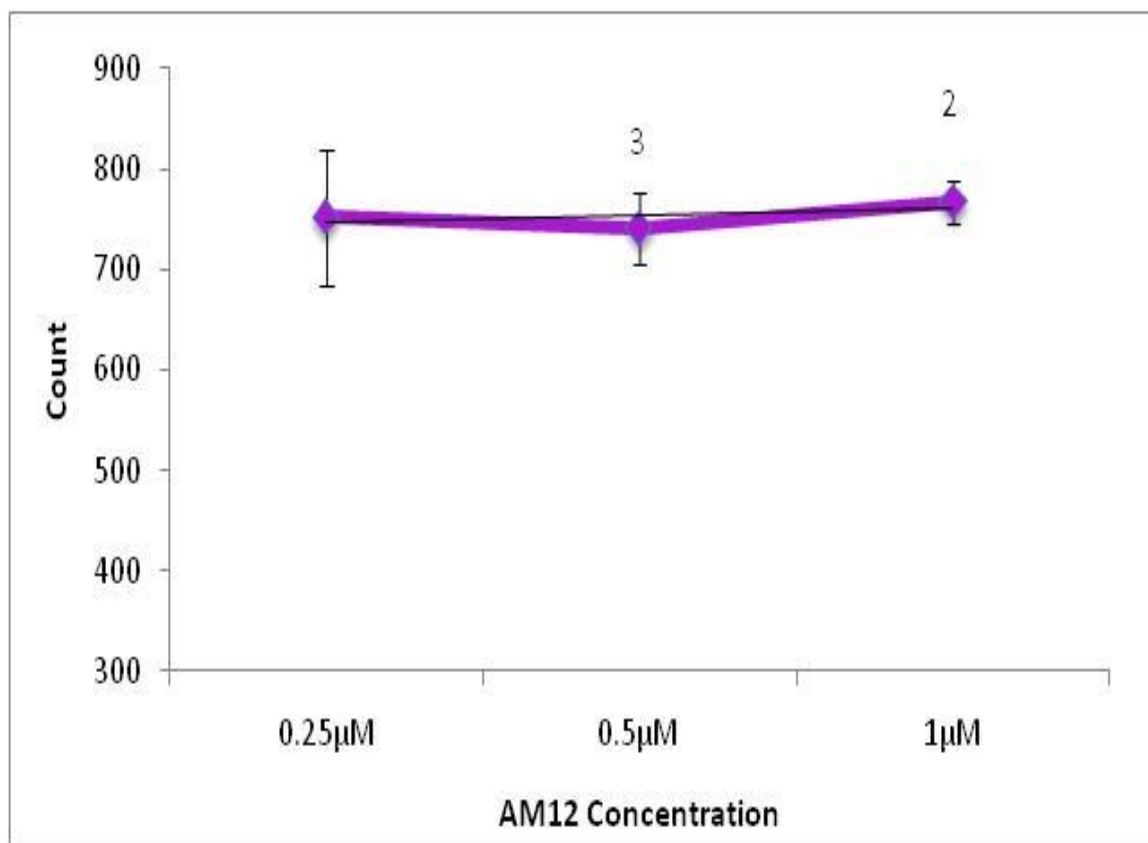


Figure 15 A549 cells were treated with increasing doses of AM12 and percentage of area covered by migrated cells was determined after 72 hours. Data was quantified using the “Custom Image J Technique.”

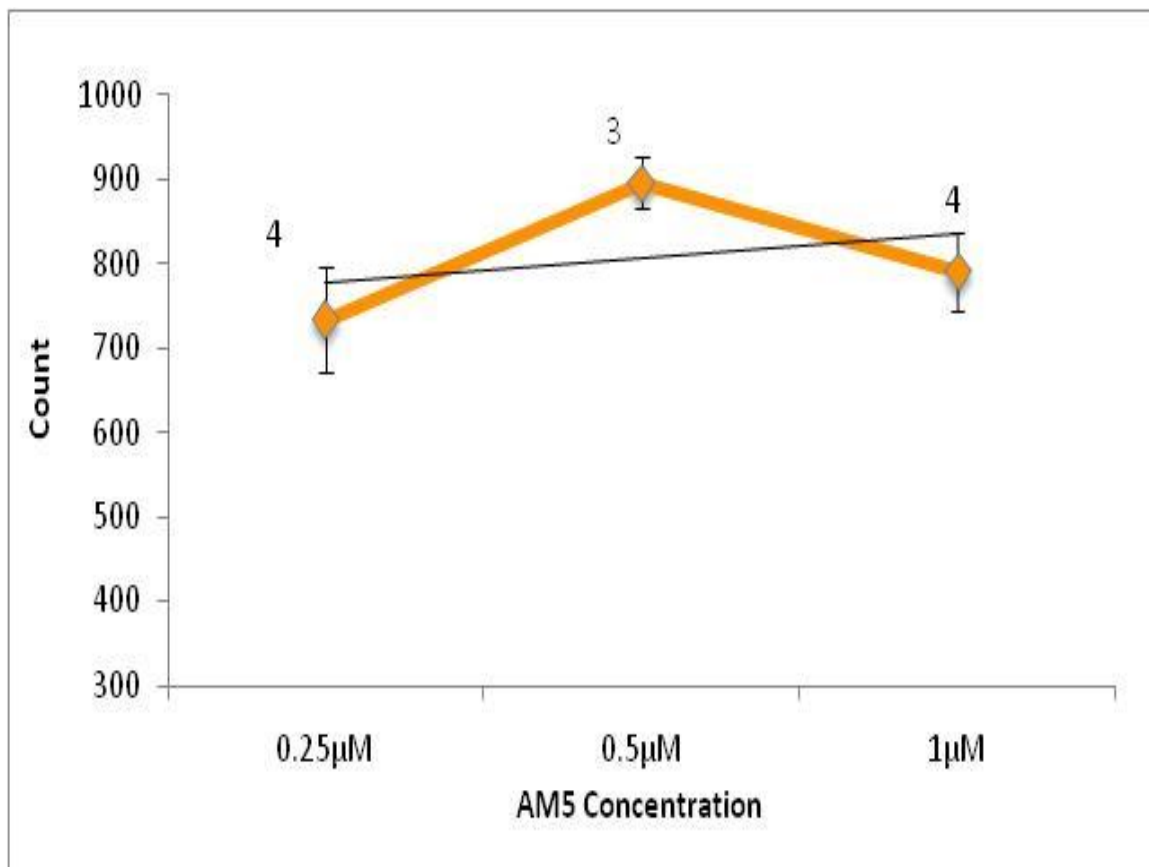


Figure 16 A549 cells were treated with increasing doses of AM5 and percentage of area covered by migrated cells was determined after 72 hours. Data was quantified using the “Custom Image J Technique.”

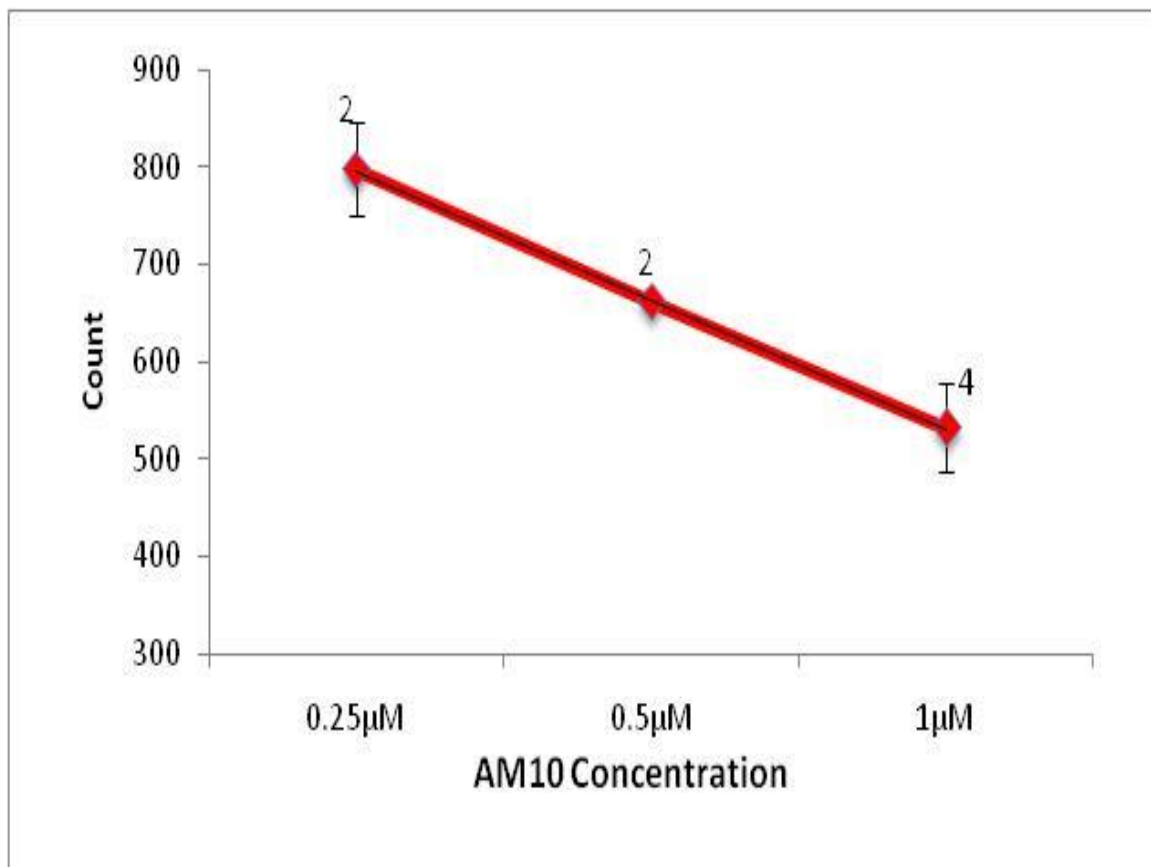


Figure 17 A549 cells were treated with increasing doses of AM10 and percentage of area covered by migrated cells was determined after 72 hours. Data was quantified using the “Custom Image J Technique.”

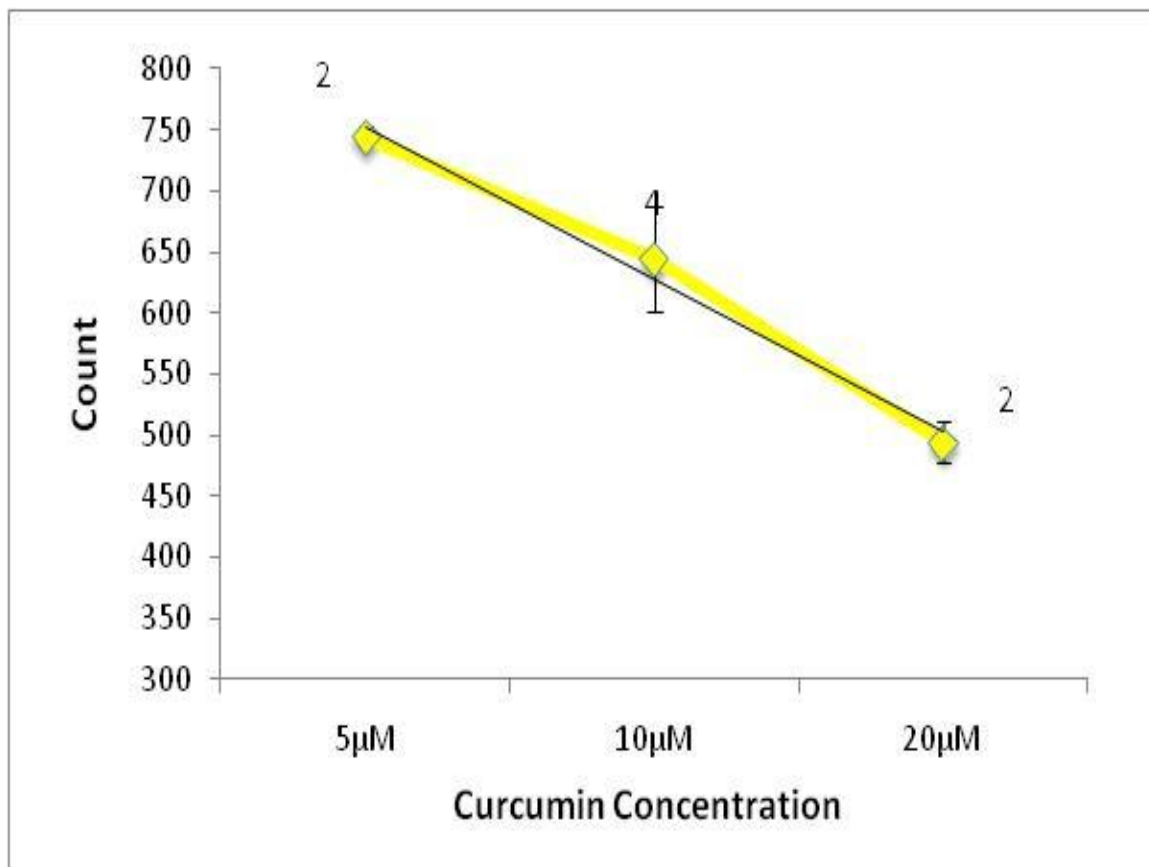


Figure 18 A549 cells were treated with increasing doses of curcumin and percentage of area covered by migrated cells was determined after 72 hours. Data was quantified using the “Custom Image J Technique.”

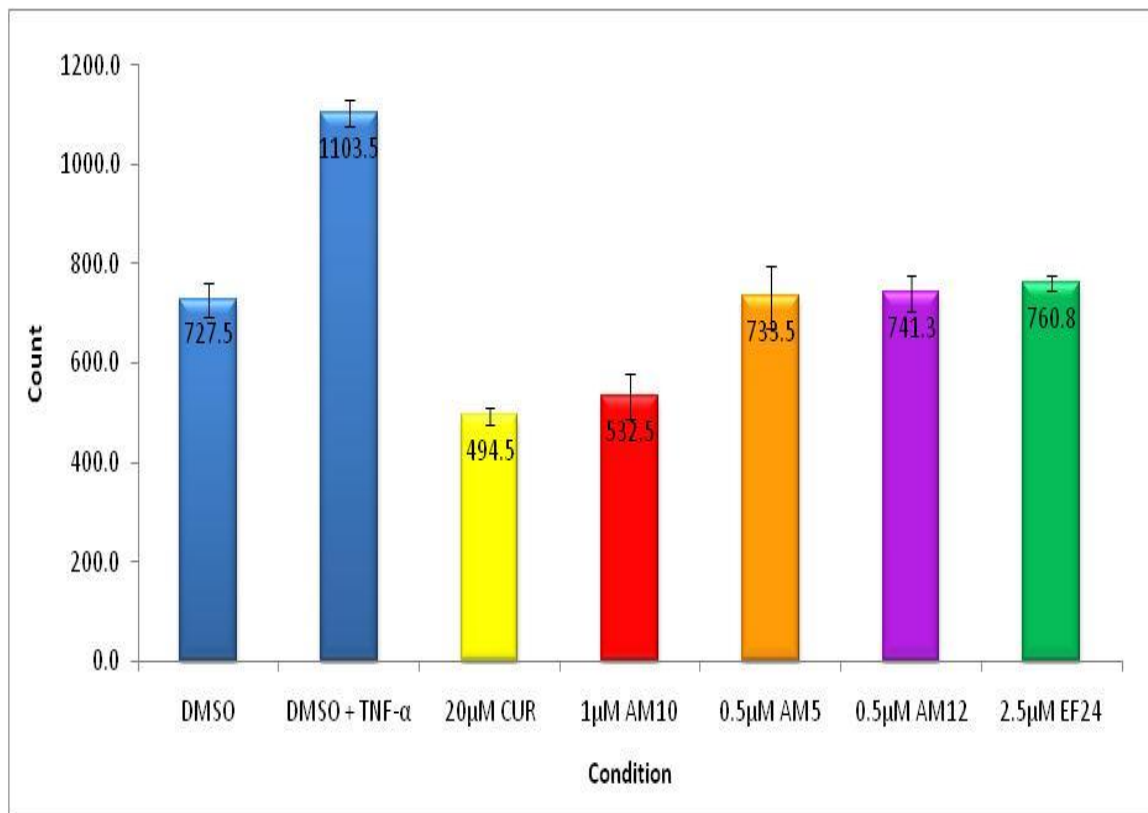


Figure 19 Each drug at the concentration that showed the greatest decrease in migrated cell count in comparison to control wells. The y-axis indicates the number of cells migrated into the detection zone. Data was quantified using the “Custom Image J Technique.”

Chapter 4: DISCUSSION

4.1 The Initial Optimization of Assay Conditions

The Oris™ cell migration assay 96-well plate is available in three different coatings of the plate surface including: tissue culture treated, collagen I and fibronectin. To determine the ideal coating for the migration assay in this study, the Oris™ Tricoated cell migration assay was purchased. The “Tricoated” plate combines three kits in one, and is ideal for assay development and evaluation of the ideal surface coating for the cell-migration application. The single 96-well plate is prepared with the three different coatings, four columns of each type. The Tricoated assay was run with cells seeded at 40,000 cells per well and 50µL which produced uneven seeding (a result which will be discussed in further detail). As a result there was no evidence migration into the detection zone. Consequently, the ideal plate coating had to be determined from literature citing of the effects of the major component of each surface coating on the migratory potential of cells. It has been well documented in the literature that collagen I plays an important role not only in migration, but also in inflammation and tumor progression (Pasco, Ramont, Maquart, & Monboisse, 2003).

Initially, 40,000 A549 cells per well was seeded in the Oris™™ cell migration assay 96-well plate. This density was selected based on data from Oris™™ website. In Figure 2 Image A, Cells were suspended in 50µL of media per well for ease in the dilution of reagents added to wells – eventually the total volume in the well would be topped off to 100µL as suggested in the product protocol. However, the resulting cell seeding was lopsided.

Cells were seeded with the stoppers in place. The pipette tip was inserted into one of two narrow ports found along either side the stoppers. The image depicts a semicircular region where the cells are most dense – this aligns with port through which the cells were pipetted. The 50 μ L volume was too low for the suspension to flow around the entire circumference of the stopper, resulting in a smaller patch opposite of the denser region in which few to no cells were localized. This uneven seeding of cells was the case in all wells even after lightly tapping the plate on the work surface as the protocol suggests. As a result, cells never reached confluence around the periphery of the detection zone and no migration was observed.

Next, a density of 40,000 cells/well and 100 μ L (not depicted) was attempted in order to circumvent the issue of uneven seeding in initial trials. 100 μ L was ideal for even seeding of cells – there was enough liquid to flow completely around the stopper region which resulted in even seeding. To further enhance this evenness, the plate was subsequently centrifuged at 1200 rpm for 1minute after seeding. However at 40,000 cells/well, a period longer than the ideal 24 hours was the required for incubation time for growth.

Consequently the cell density was increase to 50,000 cells per well as depicted in Image B. However the issue of incubation time still persisted. Specifically after seeding, cells were incubated for growth for 48 hours to reach confluence. This was not ideal as it lengthens the total time required for the assay: 48 hours of growth plus 72 hours of migration equaling a time-consuming five days. This undesired result impedes rapid data capture.

In an attempt to speed up the time required for the assay, cells were seeded at 100 μ L and 100,000 cells per well. This exceedingly high density was selected based off of the protocol of an alternative version of the Oris™ Migration Assay – Oris™ Pro which does not require overnight incubation of cells. Though this density indeed shortened time required to reach confluence; cells grew to be overly confluent before the conclusion of the experiment. The 72 hour incubation time for migration was retained as the increased confluence did not appear to induce more significant induction of migration. Consequently the cells began peel away in sheets (as depicted in Image C) disrupting the crucial pattern of the circular detection zone and surrounding periphery. This prevented data collection and analysis. Cell peeling was most likely due to effects of contact inhibition. In later experiments 60,000 cells/well and 100 μ L was found to be the optimal condition for the Oris™ cell migration assay, resulting in even seeding and a 24hr incubation time.

Subsequently the technique for addition and removal of reagents was determined, specifically for washing the cells with PBS after stopper removal. Stopper removed resulted in the creation of the region of interest in which no cells were seeded. However this process was imperfect and rogue cells fall into the center of the region and other cells become detached. As a result the media must be removed; wells washed with PBS; and fresh media replaced in the wells. The pipette scratch in Figure 3 occurred from the removal of media using the multi-channel pipette. The uniform circular monolayer is crucial for assay effectiveness and must remain intact. Disruption of the periphery has minimal effect, but disruption of the detection zone (as in Figure 3) hinders accurate data collection and analysis. As a result the protocol was modified, pipetting was used only for

the addition of reagents. All reagents were removed by physically inverting the plate and dumping out the contents of the well.

Migration of both A549 cells was slow, and migrated cells did not cover the entire detection zone despite serum starvation and subsequent the stimulation of cells with TNF- α . As a result the incubation time for migration was extended from the suggested 48 hours to 72 hours.

Imaging specifics had to be determined and optimized as well. The parameters of the <plate acquisition set-up> on the MetXpress software of the IX5000 had to be optimized for imaging of the Oris™ cell migration assay 96-well plate. Plate settings had to be customized as the Oris™ 96-well plate was not available as one of the default plate setting pre-loaded into the software. Plate dimensions were determined from the Oris™ cell migration assay protocol. Simple conversions of units were performed and entered into the relevant sections. “Distance between wells” in the Oris™ protocol corresponded to <column spacing> in the <plate acquisition set up>. <Plate length> and <Plate width> remained at the default setting for a NUNC 96-wellplate. “Offset of Wells (A-1 location, X)” and “Offset of Wells (A-1 location, Y)” correspond to <column offset> and <row offset> respectively. “Distance between Wells” corresponded to both <column spacing> and <row spacing>. “Thickness of Well Bottom” corresponded to <optical thickness>. Lastly <bottom variation> remained at the default setting for a NUNC 96-wellplate.

Similarly, the <Objective and Camera> was set to the lowest magnification in order to capture the entire well including the detection zone and periphery. Skip find sample was selected to ensure the IX5000 retained the settings and any minor

modifications made prior to acquisition of the entire plate. For a 1:5000 dilution of Hoechst 33258, <Exposure> was set to 6ms.

4.2 Initial Trials and Data Analysis Techniques

A crucial step in assay development was determining the most accurate and efficient method of data analysis. The first method attempted (depicted in Figure 7) utilized MetaXpress software and involved creating of a region of interest around the detection zone (ROI), thresholding migrated cells inside the ROI and measuring the area covered by that threshold. Specifically, this area was recorded by selecting <Region> from the <Measure> tab, and values are recorded from the column labeled “Threshold Area” or “Threshold Area Percent.” Either readout resulted in the same graphical trends, but on differing scales for the y-axis. For simplicity “Threshold Area Percent” was used as a readout – it measured the percentage of the total area of the detection zone covered by migrated cells.

The “rogue cells” mentioned previously that mistakenly become lodged in the center of the collagen matrix sometimes remain even after washing with PBS. In wells with a significant number of rogue cells, this flaw had to be accounted for in data analysis to preserve the integrity of results. Consequently, a second circular ROI was created in the center of the well excluding the cells that truly migrated into the detection zone and including the rogue cells in the center (as shown in Figure 7, Image D). The true ROI including the migrated cells was then subtracted from the ROI including the rogue cells to achieve an adjusted more correct measurement of threshold area.

Data analysis for Figures 10-13 were performed using the aforementioned “Manual MetaXpress Analysis Technique.” The migratory potential of A549 cells was lower than expected. In control wells migrated cells covered a just over 50% of the total area of the detection zone. As a result the assay window was undesirably small. Literature from the Oris™ website showed similar results (Smith et al., 2008).

When cells were treated with increasing concentrations of curcumin, the expected decrease in threshold area percentage with increasing concentration of drug was not observed. This absence of this trend also existed with EF24 treatment and was even more pronounced with a nearly flat line of best fit. The absence of a dose response curve could be attributed to a number of factors including an unfavorably small assay window. These results also suggest that the “MetaXpress Manual Technique” data analysis method was not sensitive enough to pick up subtle but significant differences in migration between conditions.

Also there was more variability at higher drug dosages in the curcumin dosage response experiment. This could again be due to the smallness of the assay window or the insensitivity of the data analysis technique. However if results are in fact accurate, the effect in question could be due to the cytotoxic effect of curcumin. At higher concentrations, curcumin may have induced apoptosis in some of the cells. This possibly resulted in a lesser more variable number of cells in total, and correspondingly more variable migration into the detection zone. This effect could have produced more inconsistency in outcomes. Further experimentation would be required to test this hypothesis. A kinetic assay would have to be performed in which total cell number could be quantified at time zero and at the endpoint of the cell migration assay.

In the same way, it was surprising that a statistically significant decrease in migration was observed at the highest concentration of curcumin in the parent compound but observed in treatment with its more potent daughter EF24. However, it is important to note that the concentration of curcumin used was 20 μ M, right at the IC₅₀ of the drug, the decrease seen though significant was slight. On the contrary 1 μ M EF24 was used, a concentration slightly lower than its IC₅₀ value of 1.3 for A549 cells (Kasinski, et al., 2008).

Experiments in Figures 10-13 each were performed in duplicate or triplicate. Also, for each one trial was run. Further trials were not run because of the less than ideal experimental conditions. Overall the lack of the expected dosage response and inhibitory potential on migration by EF24 was most likely due to the smallness of the assay window and an insensitive data analysis technique.

4.3 Further Optimization and Pilot Screen

All these results prompted further optimization of cell culture conditions to more strongly induce migration as well as to utilize a more sensitive data analysis technique. Serum starvation and stimulation were both considered as possible options to enhance migration. It was documented on the Platypus website that upon stimulation with hepatocyte growth factor (HGF) the entire detection zone was covered by A549 cell migration. A549 cells were seeded onto an Oris™ Collagen I coated, 96-well plate and allowed to adhere overnight in the presence of 10% FBS. Stoppers were removed and media containing 0.5% FBS was added. Wells were pretreated with compound for 4

hours then HGF (40 ng/mL) was added, and the plate was incubated for 48 hours to permit cell migration (Smith, et al., 2008).

In addition, researchers have found that IL-1 β induced A549 cell migration. A549 cells were cultured to confluence in six-well plates and starved with serum-free DMEM/F-12 medium for 24 h. The monolayer of cells were scratched, then serum-free DMEM/F-12 medium with or without IL-1 β was added to each dish as indicated after pretreatment with compound (Lin et al., 2009).

The stimulatory agent was chosen based off the working model of the Nf κ B pathway as it relates to the mechanism of EF24. The pathway is activated by TNF- α , IL-1 β , and Lipopolysaccharide (LPS). Though work by Smith et al showed that IL-1 β induced A549 cell migration, experiments performed by Kasinski et al to elucidate EF24's mechanism of action all involved stimulation with TNF- α at 10ng/mL. Furthermore TNF- α , IL-4 and IL-1 β together were show to stimulate A549 cell migration in a paper examining the effects of a plant extract Moutan Cortex Radicis (MCR) (J. Kim et al., 2007).

Moreover, the exact protocol for serum starvation and/or stimulation had to be determined. A serum starvation protocol modeled from both Smith et al (percentage of FBS) and Lin et al (starvation upon seeding and stimulation) was first attempted. Cells were seeded into the Oris™ 96-well plate in serum containing 0.5% FBS. Cells were allowed to adhere for 24 hours. After stopper removal and washing, fresh media containing 0.5% FBS was added. TNF- α at 10ng/mL was added after 4 hours of pre-treatment with compound. However, cells appeared to become unhealthy upon 24 hours of serum starvation and began to peel away.

Consequently stimulation in Figures 14-19 were performed without serum starvation. Cells were seeded in 10% FBS according to standard protocol, pretreated with compound for 4hours and then stimulated with TNF- α at 10ng/mL. Cells were then allowed to migrate for 72 hours.

Additionally, the data analysis protocol was further optimized. ImageJ software provided an alternative method for analysis. The basis for the steps for analysis was obtained from an application note found on the Oris™ website. This method involved, thresholding cells, creating a region of interest from the circular plate mask aperture, and analyzing particles.

The aforementioned “Platypus ImageJ Technique” was not effective for images that were especially bright or overexposed. In addition, manipulation of stoppers in the Oris™ 96-well plate can result in the warping of the bottom of the plate – this makes the analysis of Images especially difficult. Such analysis of warped plates could not be performed using the aforementioned technique. As a result a new technique was designed – the “Custom ImageJ Technique.”

The <recorder> function was used to create a Macros. Several functions were added including <Find Edges> and <Enhance Contrast>. Manual commands were carried out where the line breaks exist as show in Image B, Figure 9. Thresholding was variable from well to well and needed to be checked by eye. Often times the <Auto Threshold> function was executed manually and the lower limit was decreased so that all cells were illuminated by the indicative threshold color. The second line bread illustrates the point at which one ensured that the region of interest was the correct size and in the correct position for each well by visual inspection.

Both methods of analysis utilizing ImageJ are potentially more sensitive than the “MetaXpress Manual Technique” as they provide an actual count of the cells that have migrated into the detection zone versus a more general calculation of area covered. However the major drawback of both ImageJ analysis techniques is that the software cannot be run in batch mode with a folder of images, i.e. the software is not suitable for high-throughput applications such as our high-content screen. As a result analyses were performed individually, on a well by well basis. This process though more sensitive, is painstakingly slow and impedes rapid data collection. The ideal data analysis method would be a customized journal created using ImageXpress software that would perform the same functions of ImageJ analysis, but would automatically analyze all 96 wells simultaneously. The technical support from Molecular Devices® was not available for this study and further investigation is necessary to employ this technique.

Figure 14 showed the effects of TNF- α stimulation on migration. The entire area of the detection zone was not covered and migration time was extended to 72 hours in comparison to HGF-stimulation which resulted in full coverage and 48 hours for migration (Smith, et al., 2008). Nonetheless the assay window was successfully widened in comparison to initial trial runs. There was a statistically significant increase in the DMSO condition in comparison to DMSO+TNF- α .

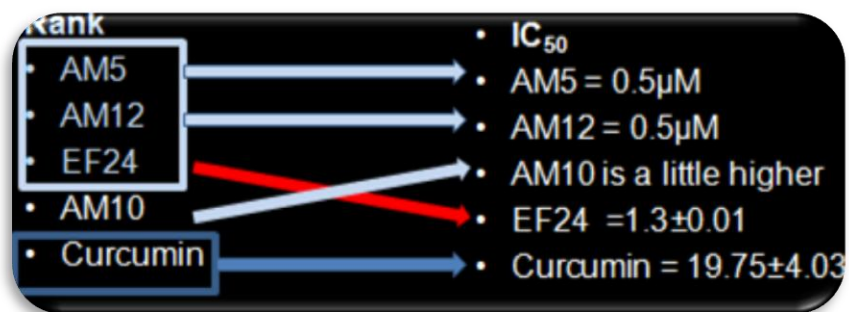
The AM- compounds are novel analogues of curcumin, hypothesized to be more potent than EF24. All compounds tested showed a statistically significant decrease in migratory potential in comparison to DMSO+TNF- α .

In dosage response experiments EF24, AM12 and AM5 did not exhibit the linear decrease expected with increasing concentrations. For EF24 and AM5 the lowest

concentrations were ideal, while for AM12 the intermediate concentration was ideal. Still the best fit lines for all 3 plots were characterized by relatively flat slopes. These three compounds were less effective than both curcumin and AM10.

AM10 and curcumin did exhibit the linear decrease expected with increasing concentrations. This result was unexpected because EF24 has been proven to be the “more potent” daughter of curcumin. In the same way, AM12 and AM5 have been hypothesized to be more potent than EF24. Consequently it was also unpredicted that curcumin would be more effective than the two compounds. It is surprising that the effects of migratory inhibition by the compounds do not mirror their cytotoxicity effects.

Interestingly one can begin to align the IC_{50} values of the drugs with their rank order based on migratory potential(considering the fact that AM5, AM12 and EF24 are not statistically different). However, EF24 breaks this trend, and if removed from the list the rank orders and the IC_{50} values align perfectly as depicted below.



At this point further conclusions cannot be drawn on the results of the AM-compounds as their structures are unpublished. However further conclusions can be drawn about the unanticipated effects of curcumin and EF24 on migration. EF-24 acts through an Nf- κ B dependent mechanism. The most direct links to Nf- κ B and metastasis and specifically migration involve the epithelial-mesenchymal transition (Karin, 2006a). However, controversy remains as to whether EMT truly happens and how important it is to metastasis (Tsuji et al., 2008). Ironically, this ambiguity may elucidate the very reason for the unexpected results. If EMT is essential to metastasis the EF-24 Nf- κ B directed mechanism would not have significant effects on cell migration.

Numerous properties have been discussed in depth in the introduction of this work that may account for curcumin surfacing as the leading compound in the rank, specifically its role as an anti-metastatic agent in the literature (S. Aggarwal, et al., 2006; Bachmeier, et al., 2007; Kunnumakkara, et al., 2009).

One to two trials of experiments in Figure 14 - 19 with 2 -5 replicates of each condition were performed. Further trials need to be run to validate these results.

CHAPTER 4: Conclusion

In conclusion, the Oris™ Cell Migration Assay imaged with the IX5000 is a feasible methodology for the phenotypic image-based screen for novel curcumin analogues with the ability to robustly inhibit migration. This application of the cell migration assay can be expanded to determine the effect of other perturbational controls to induce migration to widen the assay window and to test the efficacy wide range of diverse small molecule leads. Curcumin surfaced as the leading ranked compound with more effective inhibition of migratory potential in comparison its daughter analogues proven to have more cytotoxic effects. Further studies are necessary to elucidate the exact rationale for these unexpected results. Nonetheless “CUREcumin” has once again astonishingly proven itself a “miracle drug.”

REFERENCES

- Adams, B. K., Cai, J., Armstrong, J., Herold, M., Lu, Y. J., Sun, A., et al. (2005). EF24, a novel synthetic curcumin analog, induces apoptosis in cancer cells via a redox-dependent mechanism. *Anticancer Drugs*, 16(3), 263-275.
- Adams, B. K., Ferstl, E. M., Davis, M. C., Herold, M., Kurtkaya, S., Camalier, R. F., et al. (2004). Synthesis and biological evaluation of novel curcumin analogs as anti-cancer and anti-angiogenesis agents. *Bioorg Med Chem*, 12(14), 3871-3883.
- Adler, A. S., Lin, M., Horlings, H., Nuyten, D. S., van de Vijver, M. J., & Chang, H. Y. (2006). Genetic regulators of large-scale transcriptional signatures in cancer. *Nat Genet*, 38(4), 421-430.
- Aggarwal, B. B., Banerjee, S., Bharadwaj, U., Sung, B., Shishodia, S., & Sethi, G. (2007). Curcumin induces the degradation of cyclin E expression through ubiquitin-dependent pathway and up-regulates cyclin-dependent kinase inhibitors p21 and p27 in multiple human tumor cell lines. *Biochem Pharmacol*, 73(7), 1024-1032.
- Aggarwal, B. B., Kumar, A., & Bharti, A. C. (2003). Anticancer potential of curcumin: preclinical and clinical studies. *Anticancer Res*, 23(1A), 363-398.
- Aggarwal, S., Ichikawa, H., Takada, Y., Sandur, S. K., Shishodia, S., & Aggarwal, B. B. (2006). Curcumin (diferuloylmethane) down-regulates expression of cell proliferation and antiapoptotic and metastatic gene products through suppression of IkappaBalpha kinase and Akt activation. *Mol Pharmacol*, 69(1), 195-206.
- Allavena, P., Sica, A., Vecchi, A., Locati, M., Sozzani, S., & Mantovani, A. (2000). The chemokine receptor switch paradigm and dendritic cell migration: its significance in tumor tissues. *Immunological Reviews*, 177(1), 141-149.
- Amit, S., & Ben-Neriah, Y. (2003). NF-kappaB activation in cancer: a challenge for ubiquitination- and proteasome-based therapeutic approach. *Semin Cancer Biol*, 13(1), 15-28.
- Ammon, H. P., & Wahl, M. A. (1991). Pharmacology of *Curcuma longa*. *Planta Med*, 57(1), 1-7.
- Ammon, H. P. T., & Wahl, M. A. (1991). Pharmacology of *Curcuma-Longa*. *Planta Medica*, 57(1), 1-7.
- Annunziata, C. M., Davis, R. E., Demchenko, Y., Bellamy, W., Gabrea, A., Zhan, F., et al. (2007). Frequent engagement of the classical and alternative NF-kappaB pathways by diverse genetic abnormalities in multiple myeloma. *Cancer Cell*, 12(2), 115-130.
- Araujo, C. C. L., L. L. (2001). Biological activities of *Curcuma longa* L. *Mem Inst Oswaldo Cruz*, 96(5), 723-728.
- Arbiser, J. L., Klauber, N., Rohan, R., van Leeuwen, R., Huang, M. T., Fisher, C., et al. (1998). Curcumin is an in vivo inhibitor of angiogenesis. *Mol Med*, 4(6), 376-383.
- Azuine, M. A., & Bhide, S. V. (1992). Chemopreventive effect of turmeric against stomach and skin tumors induced by chemical carcinogens in Swiss mice. *Nutr Cancer*, 17(1), 77-83.
- Bachmeier, B., Nerlich, A. G., Iancu, C. M., Cilli, M., Schleicher, E., Vene, R., et al. (2007). The chemopreventive polyphenol Curcumin prevents hematogenous

- breast cancer metastases in immunodeficient mice. *Cell Physiol Biochem*, 19(1-4), 137-152.
- Baeuerle, P. A., & Henkel, T. (1994). Function and activation of NF-kappa B in the immune system. *Annu Rev Immunol*, 12, 141-179.
- Balkwill, F., & Mantovani, A. (2001). Inflammation and cancer: back to Virchow? *Lancet*, 357(9255), 539-545.
- Balogun, E., Hoque, M., Gong, P., Killeen, E., Green, C. J., Foresti, R., et al. (2003). Curcumin activates the haem oxygenase-1 gene via regulation of Nrf2 and the antioxidant-responsive element. *Biochem J*, 371(Pt 3), 887-895.
- Barnes, P. J., & Karin, M. (1997). Nuclear factor-kappaB: a pivotal transcription factor in chronic inflammatory diseases. *N Engl J Med*, 336(15), 1066-1071.
- Basseres, D. S., & Baldwin, A. S. (2006). Nuclear factor-kappaB and inhibitor of kappaB kinase pathways in oncogenic initiation and progression. *Oncogene*, 25(51), 6817-6830.
- Baumann, K. (2008). Intravasation and metastasis: Bringing up the rear. *Cell Migration Gateway*.
- Beasley, R. P., Hwang, L. Y., Lin, C. C., & Chien, C. S. (1981). Hepatocellular carcinoma and hepatitis B virus. A prospective study of 22 707 men in Taiwan. *Lancet*, 2(8256), 1129-1133.
- Beg, A. A., & Baltimore, D. (1996). An essential role for NF-kappaB in preventing TNF-alpha-induced cell death. *Science*, 274(5288), 782-784.
- Bhandarkar, S. S., & Arbiser, J. L. (2007). Curcumin as an inhibitor of angiogenesis. *Adv Exp Med Biol*, 595, 185-195.
- Bharti, A. C., Donato, N., Singh, S., & Aggarwal, B. B. (2003). Curcumin (diferuloylmethane) down-regulates the constitutive activation of nuclear factor-kappa B and Ikappa Balpha kinase in human multiple myeloma cells, leading to suppression of proliferation and induction of apoptosis. *Blood*, 101(3), 1053-1062.
- Bharti, A. C., Donato, N., Singh, S., & Aggarwal, B. B. (2003). Curcumin (diferuloylmethane) down-regulates the constitutive activation of nuclear factor-kappa B and Ikappa Balpha kinase in human multiple myeloma cells, leading to suppression of proliferation and induction of apoptosis. *Blood*, 101(3), 1053-1062.
- Bhattacharyya, S., Mandal, D., Sen, G. S., Pal, S., Banerjee, S., Lahiry, L., et al. (2007). Tumor-induced oxidative stress perturbs nuclear factor-kappaB activity-augmenting tumor necrosis factor-alpha-mediated T-cell death: protection by curcumin. *Cancer Res*, 67(1), 362-370.
- Bhaumik, S., Anjum, R., Rangaraj, N., Pardhasaradhi, B. V., & Khar, A. (1999). Curcumin mediated apoptosis in AK-5 tumor cells involves the production of reactive oxygen intermediates. *FEBS Lett*, 456(2), 311-314.
- Burke, F., Relf, M., Negus, R., & Balkwill, F. (1996). A cytokine profile of normal and malignant ovary. *Cytokine*, 8(7), 578-585.
- Calmels, S., Hainaut, P., & Ohshima, H. (1997). Nitric oxide induces conformational and functional modifications of wild-type p53 tumor suppressor protein. *Cancer Res*, 57(16), 3365-3369.

- Cartiera, M. S., Ferreira, E. C., Caputo, C., Egan, M. E., Caplan, M. J., & Saltzman, W. M. (2010). Partial correction of cystic fibrosis defects with PLGA nanoparticles encapsulating curcumin. *Mol Pharm*, 7(1), 86-93.
- Chandra, J., Samali, A., & Orrenius, S. (2000). Triggering and modulation of apoptosis by oxidative stress. *Free Radic Biol Med*, 29(3-4), 323-333.
- Chao, C. C., Hu, S., Molitor, T. W., Shaskan, E. G., & Peterson, P. K. (1992). Activated microglia mediate neuronal cell injury via a nitric oxide mechanism. *J Immunol*, 149(8), 2736-2741.
- Chearwae, W., & Bright, J. J. (2008). 15-deoxy-Delta(12,14)-prostaglandin J(2) and curcumin modulate the expression of toll-like receptors 4 and 9 in autoimmune T lymphocyte. *J Clin Immunol*, 28(5), 558-570.
- Chendil, D., Ranga, R. S., Meigooni, D., Sathishkumar, S., & Ahmed, M. M. (2004). Curcumin confers radiosensitizing effect in prostate cancer cell line PC-3. *Oncogene*, 23(8), 1599-1607.
- Cheng, A. L., Hsu, C. H., Lin, J. K., Hsu, M. M., Ho, Y. F., Shen, T. S., et al. (2001). Phase I clinical trial of curcumin, a chemopreventive agent, in patients with high-risk or pre-malignant lesions. *Anticancer Res*, 21(4B), 2895-2900.
- Cheng, Y., Ping, J., & Xu, L. M. (2007). Effects of curcumin on peroxisome proliferator-activated receptor gamma expression and nuclear translocation/redistribution in culture-activated rat hepatic stellate cells. *Chin Med J (Engl)*, 120(9), 794-801.
- Chirnomas, D., Taniguchi, T., de la Vega, M., Vaidya, A. P., Vasserman, M., Hartman, A. R., et al. (2006). Chemosensitization to cisplatin by inhibitors of the Fanconi anemia/BRCA pathway. *Mol Cancer Ther*, 5(4), 952-961.
- Cho, J. W., Lee, K. S., & Kim, C. W. (2007). Curcumin attenuates the expression of IL-1beta, IL-6, and TNF-alpha as well as cyclin E in TNF-alpha-treated HaCaT cells; NF-kappaB and MAPKs as potential upstream targets. *Int J Mol Med*, 19(3), 469-474.
- Cho, J. W., Park, K., Kweon, G. R., Jang, B. C., Baek, W. K., Suh, M. H., et al. (2005). Curcumin inhibits the expression of COX-2 in UVB-irradiated human keratinocytes (HaCaT) by inhibiting activation of AP-1: p38 MAP kinase and JNK as potential upstream targets. *Exp Mol Med*, 37(3), 186-192.
- Chua, H. L., Bhat-Nakshatri, P., Clare, S. E., Morimiya, A., Badve, S., & Nakshatri, H. (2007). NF-kappaB represses E-cadherin expression and enhances epithelial to mesenchymal transition of mammary epithelial cells: potential involvement of ZEB-1 and ZEB-2. *Oncogene*, 26(5), 711-724.
- Coomber, B. L., & Gotlieb, A. I. (1990). In vitro endothelial wound repair. Interaction of cell migration and proliferation. *Arteriosclerosis*, 10(2), 215-222.
- Cowin, P., & Welch, D. R. (2007). Breast cancer progression: controversies and consensus in the molecular mechanisms of metastasis and EMT. *J Mammary Gland Biol Neoplasia*, 12(2-3), 99-102.
- Cruz-Correa, M., Shoskes, D. A., Sanchez, P., Zhao, R., Hyland, L. M., Wexner, S. D., et al. (2006). Combination treatment with curcumin and quercetin of adenomas in familial adenomatous polyposis. *Clin Gastroenterol Hepatol*, 4(8), 1035-1038.
- Das, K. C., & Das, C. K. (2002). Curcumin (diferuloylmethane), a singlet oxygen ((1)O(2)) quencher. *Biochem Biophys Res Commun*, 295(1), 62-66.

- Daybe, F. (1870). Uber Curcumin. den Farbstoff der Curcumawurzzel. *Ber. Dtsch. Chem. Ges*, 3, 609.
- De, R., Kundu, P., Swarnakar, S., Ramamurthy, T., Chowdhury, A., Nair, G. B., et al. (2009). Antimicrobial activity of curcumin against *Helicobacter pylori* isolates from India and during infections in mice. *Antimicrob Agents Chemother*, 53(4), 1592-1597.
- Deodhar, S. D., Sethi, R., & Srimal, R. C. (1980). Preliminary study on antirheumatic activity of curcumin (diferuloyl methane). *Indian J Med Res*, 71, 632-634.
- Deshpande, S. S., Ingle, A. D., & Maru, G. B. (1997). Inhibitory effects of curcumin-free aqueous turmeric extract on benzo[a]pyrene-induced forestomach papillomas in mice. *Cancer Lett*, 118(1), 79-85.
- Dikshit, M., Rastogi, L., Shukla, R., & Srimal, R. C. (1995). Prevention of ischaemia-induced biochemical changes by curcumin & quinidine in the cat heart. *Indian J Med Res*, 101, 31-35.
- Dinkova-Kostova, A. T., Massiah, M. A., Bozak, R. E., Hicks, R. J., & Talalay, P. (2001). Potency of Michael reaction acceptors as inducers of enzymes that protect against carcinogenesis depends on their reactivity with sulfhydryl groups. *Proc Natl Acad Sci U S A*, 98(6), 3404-3409.
- Durgaprasad, S., Pai, C. G., Vasanthkumar, Alvres, J. F., & Namitha, S. (2005). A pilot study of the antioxidant effect of curcumin in tropical pancreatitis. *Indian J Med Res*, 122(4), 315-318.
- Dvorak, H. (1986). Tumors: wounds that do not heal. *N Engl J Med*, 315, 1650-1659.
- Ebnet, K., & Vestweber, D. (1999). Molecular mechanisms that control leukocyte extravasation: the selectins and the chemokines. *Histochem Cell Biol*, 112(1), 1-23.
- Fabre, C., Carvalho, G., Tasdemir, E., Braun, T., Ades, L., Grosjean, J., et al. (2007). NF-kappaB inhibition sensitizes to starvation-induced cell death in high-risk myelodysplastic syndrome and acute myeloid leukemia. *Oncogene*, 26(28), 4071-4083.
- Falzano, L., Fiorentini, C., Donelli, G., Michel, E., Kocks, C., Cossart, P., et al. (1993). Induction of phagocytic behaviour in human epithelial cells by *Escherichia coli* cytotoxic necrotizing factor type 1. *Mol Microbiol*, 9(6), 1247-1254.
- Farombi, E. O., & Ekor, M. (2006). Curcumin attenuates gentamicin-induced renal oxidative damage in rats. *Food Chem Toxicol*, 44(9), 1443-1448.
- Fischer, H. G., & Reichmann, G. (2001). Brain dendritic cells and macrophages/microglia in central nervous system inflammation. *J Immunol*, 166(4), 2717-2726.
- Frank, N., Knauft, J., Amelung, F., Nair, J., Wesch, H., & Bartsch, H. (2003). No prevention of liver and kidney tumors in Long-Evans Cinnamon rats by dietary curcumin, but inhibition at other sites and of metastases. *Mutat Res*, 523-524, 127-135.
- Gaddipati, J. P., Sundar, S. V., Calemene, J., Seth, P., Sidhu, G. S., & Maheshwari, R. K. (2003). Differential regulation of cytokines and transcription factors in liver by curcumin following hemorrhage/resuscitation. *Shock*, 19(2), 150-156.
- Gao, X., Kuo, J., Jiang, H., Deeb, D., Liu, Y., Divine, G., et al. (2004). Immunomodulatory activity of curcumin: suppression of lymphocyte

- proliferation, development of cell-mediated cytotoxicity, and cytokine production in vitro. *Biochem Pharmacol*, 68(1), 51-61.
- Garcea, G., Jones, D. J., Singh, R., Dennison, A. R., Farmer, P. B., Sharma, R. A., et al. (2004). Detection of curcumin and its metabolites in hepatic tissue and portal blood of patients following oral administration. *Br J Cancer*, 90(5), 1011-1015.
- Garg, A. K., Buchholz, T. A., & Aggarwal, B. B. (2005). Chemosensitization and radiosensitization of tumors by plant polyphenols. *Antioxid Redox Signal*, 7(11-12), 1630-1647.
- Ghosh, S., May, M. J., & Kopp, E. B. (1998). NF- κ B AND REL PROTEINS: Evolutionarily Conserved Mediators of Immune Responses. *Annual Review of Immunology*, 16(1), 225-260.
- Goel, A., Jhurani, S., & Aggarwal, B. B. (2008). Multi-targeted therapy by curcumin: how spicy is it? *Mol Nutr Food Res*, 52(9), 1010-1030.
- Goel, A., Kunnumakkara, A. B., & Aggarwal, B. B. (2008). Curcumin as "Curecumin": from kitchen to clinic. *Biochem Pharmacol*, 75(4), 787-809.
- Govindarajan, V. S. (1980). Turmeric--chemistry, technology, and quality. *Crit Rev Food Sci Nutr*, 12(3), 199-301.
- Granstein, R. D., & Matsui, M. S. (2004). UV radiation-induced immunosuppression and skin cancer. *Cutis*, 74(5 Suppl), 4-9.
- Gulumian, M. (1999). The role of oxidative stress in diseases caused by mineral dusts and fibres: current status and future of prophylaxis and treatment. *Mol Cell Biochem*, 196(1-2), 69-77.
- Hanahan, D., & Weinberg, R. A. (2000). The hallmarks of cancer. *Cell*, 100(1), 57-70.
- Hatcher, H., Planalp, R., Cho, J., Torti, F. M., & Torti, S. V. (2008). Curcumin: from ancient medicine to current clinical trials. *Cell Mol Life Sci*, 65(11), 1631-1652.
- Heng, M. C., Song, M. K., Harker, J., & Heng, M. K. (2000). Drug-induced suppression of phosphorylase kinase activity correlates with resolution of psoriasis as assessed by clinical, histological and immunohistochemical parameters. *Br J Dermatol*, 143(5), 937-949.
- Hidaka, H., Ishiko, T., Furuhashi, T., Kamohara, H., Suzuki, S., Miyazaki, M., et al. (2002). Curcumin inhibits interleukin 8 production and enhances interleukin 8 receptor expression on the cell surface. *Cancer*, 95(6), 1206-1214.
- Holder, G. M., Plummer, J. L., & Ryan, A. J. (1978). The metabolism and excretion of curcumin (1,7-bis-(4-hydroxy-3-methoxyphenyl)-1,6-heptadiene-3,5-dione) in the rat. *Xenobiotica*, 8(12), 761-768.
- Holt, P. R., Katz, S., & Kirshoff, R. (2005). Curcumin therapy in inflammatory bowel disease: a pilot study. *Dig Dis Sci*, 50(11), 2191-2193.
- Honn, K. V., Grossi, I. M., Steinert, B. W., Chopra, H., Onoda, J., Nelson, K. K., et al. (1989). Lipoxygenase regulation of membrane expression of tumor cell glycoproteins and subsequent metastasis. *Adv Prostaglandin Thromboxane Leukot Res*, 19, 439-443.
- Horikawa, T., Yang, J., Kondo, S., Yoshizaki, T., Joab, I., Furukawa, M., et al. (2007). Twist and epithelial-mesenchymal transition are induced by the EBV oncoprotein latent membrane protein 1 and are associated with metastatic nasopharyngeal carcinoma. *Cancer Res*, 67(5), 1970-1978.

- Huang, M. T., Lysz, T., Ferraro, T., Abidi, T. F., Laskin, J. D., & Conney, A. H. (1991). Inhibitory effects of curcumin on in vitro lipoxygenase and cyclooxygenase activities in mouse epidermis. *Cancer Res*, *51*(3), 813-819.
- Huber, M. A., Azoitei, N., Baumann, B., Grunert, S., Sommer, A., Pehamberger, H., et al. (2004). NF-kappaB is essential for epithelial-mesenchymal transition and metastasis in a model of breast cancer progression. *J Clin Invest*, *114*(4), 569-581.
- Ireson, C. R., Jones, D. J., Orr, S., Coughtrie, M. W., Boocock, D. J., Williams, M. L., et al. (2002). Metabolism of the cancer chemopreventive agent curcumin in human and rat intestine. *Cancer Epidemiol Biomarkers Prev*, *11*(1), 105-111.
- Jagetia, G. C. (2007). Radioprotection and radiosensitization by curcumin. *Adv Exp Med Biol*, *595*, 301-320.
- Joe, B., Vijaykumar, M., & Lokesh, B. R. (2004). Biological properties of curcumin-cellular and molecular mechanisms of action. *Crit Rev Food Sci Nutr*, *44*(2), 97-111.
- Karin, M. (2006a). NF-kappaB and cancer: mechanisms and targets. *Mol Carcinog*, *45*(6), 355-361.
- Karin, M. (2006b). Nuclear factor-kappaB in cancer development and progression. *Nature*, *441*(7092), 431-436.
- Karin, M., Cao, Y., Greten, F. R., & Li, Z. W. (2002). NF-kappaB in cancer: from innocent bystander to major culprit. *Nat Rev Cancer*, *2*(4), 301-310.
- Kasinski, A. L., Du, Y., Thomas, S. L., Zhao, J., Sun, S. Y., Khuri, F. R., et al. (2008). Inhibition of IkappaB kinase-nuclear factor-kappaB signaling pathway by 3,5-bis(2-fluorobenzylidene)piperidin-4-one (EF24), a novel monoketone analog of curcumin. *Mol Pharmacol*, *74*(3), 654-661.
- Kidd, P. M. (2009). Bioavailability and activity of phytosome complexes from botanical polyphenols: the silymarin, curcumin, green tea, and grape seed extracts. *Altern Med Rev*, *14*(3), 226-246.
- Kim, H. Y., Park, E. J., Joe, E. H., & Jou, I. (2003). Curcumin suppresses Janus kinase-STAT inflammatory signaling through activation of Src homology 2 domain-containing tyrosine phosphatase 2 in brain microglia. *J Immunol*, *171*(11), 6072-6079.
- Kim, J., Lee, H., Lee, Y., Oh, B. G., Cho, C., Kim, Y., et al. (2007). Inhibition effects of Moutan Cortex Radicis on secretion of eotaxin in A549 human epithelial cells and eosinophil migration. *J Ethnopharmacol*, *114*(2), 186-193.
- Kiso, Y., Suzuki, Y., Watanabe, N., Oshima, Y., & Hikino, H. (1983). Antihepatotoxic principles of *Curcuma longa* rhizomes. *Planta Med*, *49*(3), 185-187.
- Kobayashi, H., Boelte, K. C., & Lin, P. C. (2007). Endothelial cell adhesion molecules and cancer progression. *Curr Med Chem*, *14*(4), 377-386.
- Kunnumakkara, A. B., Diagaradjane, P., Anand, P., Harikumar, K. B., Deorukhkar, A., Gelovani, J., et al. (2009). Curcumin sensitizes human colorectal cancer to capecitabine by modulation of cyclin D1, COX-2, MMP-9, VEGF and CXCR4 expression in an orthotopic mouse model. *Int J Cancer*, *125*(9), 2187-2197.
- Kuper, H., Adami, H. O., & Trichopoulos, D. (2000). Infections as a major preventable cause of human cancer. *J Intern Med*, *248*(3), 171-183.
- Kutluay, S. B., Doroghazi, J., Roemer, M. E., & Triezenberg, S. J. (2008). Curcumin inhibits herpes simplex virus immediate-early gene expression by a mechanism

- independent of p300/CBP histone acetyltransferase activity. *Virology*, 373(2), 239-247.
- Kuttan, R., Sudheeran, P. C., & Josph, C. D. (1987). Turmeric and curcumin as topical agents in cancer therapy. *Tumori*, 73(1), 29-31.
- Lal, B., Kapoor, A. K., Agrawal, P. K., Asthana, O. P., & Srimal, R. C. (2000). Role of curcumin in idiopathic inflammatory orbital pseudotumours. *Phytother Res*, 14(6), 443-447.
- Lal, B., Kapoor, A. K., Asthana, O. P., Agrawal, P. K., Prasad, R., Kumar, P., et al. (1999). Efficacy of curcumin in the management of chronic anterior uveitis. *Phytother Res*, 13(4), 318-322.
- Lao, C. D., Ruffin, M. T. t., Normolle, D., Heath, D. D., Murray, S. I., Bailey, J. M., et al. (2006). Dose escalation of a curcuminoid formulation. *BMC Complement Altern Med*, 6, 10.
- Lee, S. J., & Benveniste, E. N. (1999). Adhesion molecule expression and regulation on cells of the central nervous system. *J Neuroimmunol*, 98(2), 77-88.
- Levin, I. (1913). The Mechanisms of Metastasis Formation in Experimental Cancer. *J Exp Med*, 18(4), 397-405.
- Li, M., Zhang, Z., Hill, D. L., Wang, H., & Zhang, R. (2007). Curcumin, a dietary component, has anticancer, chemosensitization, and radiosensitization effects by down-regulating the MDM2 oncogene through the PI3K/mTOR/ETS2 pathway. *Cancer Res*, 67(5), 1988-1996.
- Lim, G. P., Chu, T., Yang, F., Beech, W., Frautschy, S. A., & Cole, G. M. (2001). The curry spice curcumin reduces oxidative damage and amyloid pathology in an Alzheimer transgenic mouse. *J Neurosci*, 21(21), 8370-8377.
- Limtrakul, P., Lipigorngoson, S., Namwong, O., Apisariyakul, A., & Dunn, F. W. (1997). Inhibitory effect of dietary curcumin on skin carcinogenesis in mice. *Cancer Lett*, 116(2), 197-203.
- Lin, C. C., Kuo, C. T., Cheng, C. Y., Wu, C. Y., Lee, C. W., Hsieh, H. L., et al. (2009). IL-1 beta promotes A549 cell migration via MAPKs/AP-1- and NF-kappaB-dependent matrix metalloproteinase-9 expression. *Cell Signal*, 21(11), 1652-1662.
- Literat, A., Su, F., Norwicki, M., Durand, M., Ramanathan, R., Jones, C. A., et al. (2001). Regulation of pro-inflammatory cytokine expression by curcumin in hyaline membrane disease (HMD). *Life Sci*, 70(3), 253-267.
- Lopez-Lazaro, M. (2008). Anticancer and carcinogenic properties of curcumin: considerations for its clinical development as a cancer chemopreventive and chemotherapeutic agent. *Mol Nutr Food Res*, 52 Suppl 1, S103-127.
- Luo, J. L., Tan, W., Ricono, J. M., Korchynskiy, O., Zhang, M., Gonias, S. L., et al. (2007). Nuclear cytokine-activated IKKalpha controls prostate cancer metastasis by repressing Maspin. *Nature*, 446(7136), 690-694.
- Ma, Q. L., Yang, F., Rosario, E. R., Ubeda, O. J., Beech, W., Gant, D. J., et al. (2009). Beta-amyloid oligomers induce phosphorylation of tau and inactivation of insulin receptor substrate via c-Jun N-terminal kinase signaling: suppression by omega-3 fatty acids and curcumin. *J Neurosci*, 29(28), 9078-9089.
- MacGregor, H. (2006). Out of the spice box, into the lab: Turmeric, an Indian staple, has long had medicinal uses. Now the West is taking notice. *Los Angeles Times*.

- Maheshwari, R. K., Singh, A. K., Gaddipati, J., & Srimal, R. C. (2006). Multiple biological activities of curcumin: a short review. *Life Sci*, 78(18), 2081-2087.
- Manjunatha, H., & Srinivasan, K. (2007). Hypolipidemic and antioxidant effects of dietary curcumin and capsaicin in induced hypercholesterolemic rats. *Lipids*, 42(12), 1133-1142.
- Mantovani, A., Bottazzi, B., Colotta, F., Sozzani, S., & Ruco, L. (1992). The origin and function of tumor-associated macrophages. *Immunol Today*, 13(7), 265-270.
- Mantovani, A., Bussolino, F., & Dejana, E. (1992). Cytokine regulation of endothelial cell function. *FASEB J*, 6(8), 2591-2599.
- Marczylo, T., Verschoyle, R., Cooke, D., Morazzoni, P., Steward, W., & Gescher, A. (2007). Comparison of systemic availability of curcumin with that of curcumin formulated with phosphatidylcholine. [10.1007/s00280-006-0355-x]. *Cancer Chemotherapy and Pharmacology*, 60(2), 171-177.
- Marnett, L. J. (1992). Aspirin and the potential role of prostaglandins in colon cancer. *Cancer Res*, 52(20), 5575-5589.
- Mathew AG, P. S. *Indian Spices*. Kerala, India.
- Mc Henry, K. T., Ankala, S. V., Ghosh, A. K., & Fenteany, G. (2002). A non-antibacterial oxazolidinone derivative that inhibits epithelial cell sheet migration. *Chembiochem*, 3(11), 1105-1111.
- Mehta, K., Pantazis, P., McQueen, T., & Aggarwal, B. B. (1997). Antiproliferative effect of curcumin (diferuloylmethane) against human breast tumor cell lines. *Anticancer Drugs*, 8(5), 470-481.
- Menon, L. G., Kuttan, R., & Kuttan, G. (1995). Inhibition of lung metastasis in mice induced by B16F10 melanoma cells by polyphenolic compounds. *Cancer Lett*, 95(1-2), 221-225.
- Milobedzka, J., v. Kostanecki, S. and Lampe, V. (1910). Curcumin. *Ber. Dtsch. Chem. Ges*, 43, 2163-2170.
- Mizoguchi, H., O'Shea, J. J., Longo, D. L., Loeffler, C. M., McVicar, D. W., & Ochoa, A. C. (1992). Alterations in signal transduction molecules in T lymphocytes from tumor-bearing mice. *Science*, 258(5089), 1795-1798.
- Motterlini, R., Foresti, R., Bassi, R., & Green, C. J. (2000). Curcumin, an antioxidant and anti-inflammatory agent, induces heme oxygenase-1 and protects endothelial cells against oxidative stress. *Free Radic Biol Med*, 28(8), 1303-1312.
- Mukhopadhyay, A., Banerjee, S., Stafford, L. J., Xia, C., Liu, M., & Aggarwal, B. B. (2002). Curcumin-induced suppression of cell proliferation correlates with down-regulation of cyclin D1 expression and CDK4-mediated retinoblastoma protein phosphorylation. *Oncogene*, 21(57), 8852-8861.
- Nair, J., Strand, S., Frank, N., Knauff, J., Wesch, H., Galle, P. R., et al. (2005). Apoptosis and age-dependant induction of nuclear and mitochondrial etheno-DNA adducts in Long-Evans Cinnamon (LEC) rats: enhanced DNA damage by dietary curcumin upon copper accumulation. *Carcinogenesis*, 26(7), 1307-1315.
- Naugler, W. E., & Karin, M. (2008). NF-kappaB and cancer-identifying targets and mechanisms. *Curr Opin Genet Dev*, 18(1), 19-26.
- Negus, R. P., Stamp, G. W., Hadley, J., & Balkwill, F. R. (1997). Quantitative assessment of the leukocyte infiltrate in ovarian cancer and its relationship to the expression of C-C chemokines. *Am J Pathol*, 150(5), 1723-1734.

- Newman, D. J., Cragg, G. M., & Snader, K. M. (2003). Natural products as sources of new drugs over the period 1981-2002. *J Nat Prod*, *66*(7), 1022-1037.
- Nirmala, C., & Puvanakrishnan, R. (1996). Protective role of curcumin against isoproterenol induced myocardial infarction in rats. *Mol Cell Biochem*, *159*(2), 85-93.
- Norman, J. (1991). *The Complete Book of Spices* (Vol.). New York, NY: Studio Books, Penguin Books USA Inc.
- Novak, K. A healing process.
- Oetari, S., Sudibyo, M., Commandeur, J. N., Samhoedi, R., & Vermeulen, N. P. (1996). Effects of curcumin on cytochrome P450 and glutathione S-transferase activities in rat liver. *Biochem Pharmacol*, *51*(1), 39-45.
- Oris™ Cell Migration Assay. (2010). Retrieved 4/14/2010, from <http://www.platypustech.com/discoverAssay.html>
- Pan, M.-H., Huang, T.-M., & Lin, J.-K. (1999). Biotransformation of Curcumin Through Reduction and Glucuronidation in Mice. *Drug Metabolism and Disposition*, *27*(4), 486-494.
- Pandeya, N. (2005). Old wives tales: Modern miracles. *Trees Life J.*, *1*.
- Park, M. J., Kim, E. H., Park, I. C., Lee, H. C., Woo, S. H., Lee, J. Y., et al. (2002). Curcumin inhibits cell cycle progression of immortalized human umbilical vein endothelial (ECV304) cells by up-regulating cyclin-dependent kinase inhibitor, p21WAF1/CIP1, p27KIP1 and p53. *Int J Oncol*, *21*(2), 379-383.
- Pasco, S., Ramont, L., Maquart, F. X., & Monboisse, J. C. (2003). [Biological effects of collagen I and IV peptides]. *J Soc Biol*, *197*(1), 31-39.
- Payton, F., Sandusky, P., & Alworth, W. L. (2007). NMR study of the solution structure of curcumin. *J Nat Prod*, *70*(2), 143-146.
- Pinedo, H. M., Verheul, H. M., D'Amato, R. J., & Folkman, J. (1998). Involvement of platelets in tumour angiogenesis? *Lancet*, *352*(9142), 1775-1777.
- Piwocka, K., Jaruga, E., Skierski, J., Gradzka, I., & Sikora, E. (2001). Effect of glutathione depletion on caspase-3 independent apoptosis pathway induced by curcumin in Jurkat cells. *Free Radic Biol Med*, *31*(5), 670-678.
- Plummer, S. M., Holloway, K. A., Manson, M. M., Munks, R. J., Kaptein, A., Farrow, S., et al. (1999). Inhibition of cyclo-oxygenase 2 expression in colon cells by the chemopreventive agent curcumin involves inhibition of NF-kappaB activation via the NIK/IKK signalling complex. *Oncogene*, *18*(44), 6013-6020.
- Priyadarsini, K. I. (1997). Free radical reactions of curcumin in membrane models. *Free Radic Biol Med*, *23*(6), 838-843.
- Priyadarsini, K. I., Maity, D. K., Naik, G. H., Kumar, M. S., Unnikrishnan, M. K., Satav, J. G., et al. (2003). Role of phenolic O-H and methylene hydrogen on the free radical reactions and antioxidant activity of curcumin. *Free Radic Biol Med*, *35*(5), 475-484.
- Qureshi, S., Shah, A. H., & Ageel, A. M. (1992). Toxicity studies on *Alpinia galanga* and *Curcuma longa*. *Planta Med*, *58*(2), 124-127.
- Rae, C., Langa, S., Tucker, S. J., & MacEwan, D. J. (2007). Elevated NF-κB responses and FLIP levels in leukemic but not normal lymphocytes: reduction by salicylate allows TNF-induced apoptosis. *Proceedings of the National Academy of Sciences*, *104*(31), 12790-12795.

- Rao, C. V., Rivenson, A., Simi, B., & Reddy, B. S. (1995). Chemoprevention of colon carcinogenesis by dietary curcumin, a naturally occurring plant phenolic compound. *Cancer Res*, *55*(2), 259-266.
- Rasyid, A., & Lelo, A. (1999). The effect of curcumin and placebo on human gallbladder function: an ultrasound study. *Aliment Pharmacol Ther*, *13*(2), 245-249.
- Ravindranath, V., & Chandrasekhara, N. (1980). Absorption and tissue distribution of curcumin in rats. *Toxicology*, *16*(3), 259-265.
- Ravindranath, V., & Chandrasekhara, N. (1981). Metabolism of curcumin--studies with [3H]curcumin. *Toxicology*, *22*(4), 337-344.
- Reyes-Gordillo, K., Segovia, J., Shibayama, M., Vergara, P., Moreno, M. G., & Muriel, P. (2007). Curcumin protects against acute liver damage in the rat by inhibiting NF-kappaB, proinflammatory cytokines production and oxidative stress. *Biochim Biophys Acta*, *1770*(6), 989-996.
- Sakano, K., & Kawanishi, S. (2002). Metal-mediated DNA damage induced by curcumin in the presence of human cytochrome P450 isozymes. *Arch Biochem Biophys*, *405*(2), 223-230.
- Salh, B., Assi, K., Templeman, V., Parhar, K., Owen, D., Gomez-Munoz, A., et al. (2003). Curcumin attenuates DNB-induced murine colitis. *Am J Physiol Gastrointest Liver Physiol*, *285*(1), G235-243.
- Santibanez, J. F., Quintanilla, M., & Martinez, J. (2000). Genistein and curcumin block TGF-beta 1-induced u-PA expression and migratory and invasive phenotype in mouse epidermal keratinocytes. *Nutr Cancer*, *37*(1), 49-54.
- Scartozzi, M., Bearzi, I., Pierantoni, C., Mandolesi, A., Loupakis, F., Zaniboni, A., et al. (2007). Nuclear Factor-kB Tumor Expression Predicts Response and Survival in Irinotecan-Refractory Metastatic Colorectal Cancer Treated With Cetuximab-Irinotecan Therapy. *J Clin Oncol*, *25*(25), 3930-3935.
- Sen, R., & Baltimore, D. (1986). Inducibility of kappa immunoglobulin enhancer-binding protein Nf-kappa B by a posttranslational mechanism. *Cell*, *47*(6), 921-928.
- Senftleben, U., Cao, Y., Xiao, G., Greten, F. R., Krahn, G., Bonizzi, G., et al. (2001). Activation by IKKalpha of a Second, Evolutionary Conserved, NF-kappa B Signaling Pathway. *Science*, *293*(5534), 1495-1499.
- Shaffer, C. (2009). Cell Migration Assays. Retrieved from <http://www.biocompare.com/Articles/FeaturedArticle/1065/Cell-Migration-Assays.html>
- Shankar, T. N., Shantha, N. V., Ramesh, H. P., Murthy, I. A., & Murthy, V. S. (1980). Toxicity studies on turmeric (*Curcuma longa*): acute toxicity studies in rats, guineapigs & monkeys. *Indian J Exp Biol*, *18*(1), 73-75.
- Sharma, R. A., Euden, S. A., Platton, S. L., Cooke, D. N., Shafayat, A., Hewitt, H. R., et al. (2004). Phase I clinical trial of oral curcumin: biomarkers of systemic activity and compliance. *Clin Cancer Res*, *10*(20), 6847-6854.
- Sharma, R. A., McLelland, H. R., Hill, K. A., Ireson, C. R., Euden, S. A., Manson, M. M., et al. (2001). Pharmacodynamic and pharmacokinetic study of oral *Curcuma* extract in patients with colorectal cancer. *Clin Cancer Res*, *7*(7), 1894-1900.
- Shishodia, S., Amin, H. M., Lai, R., & Aggarwal, B. B. (2005). Curcumin (diferuloylmethane) inhibits constitutive NF-[kappa]B activation, induces G1/S

- arrest, suppresses proliferation, and induces apoptosis in mantle cell lymphoma. *Biochemical Pharmacology*, 70(5), 700-713.
- Shishodia, S., Sethi, G., & Aggarwal, B. B. (2005). Curcumin: getting back to the roots. *Ann N Y Acad Sci*, 1056, 206-217.
- Shoba, G., Joy, D., Joseph, T., Majeed, M., Rajendran, R., & Srinivas, P. S. (1998). Influence of piperine on the pharmacokinetics of curcumin in animals and human volunteers. *Planta Med*, 64(4), 353-356.
- Shukla, Y., Arora, A., & Taneja, P. (2002). Antimutagenic potential of curcumin on chromosomal aberrations in Wistar rats. *Mutat Res*, 515(1-2), 197-202.
- Siebenlist, U., Franzoso, G., & Brown, K. (1994). Structure, regulation and function of NF-kappa B. *Annu Rev Cell Biol*, 10, 405-455.
- Singh, S., & Aggarwal, B. B. (1995). Activation of Transcription Factor NF-B Is Suppressed by Curcumin (Diferuloylmethane). *Journal of Biological Chemistry*, 270(42), 24995-25000.
- Singh, S., & Khar, A. (2006). Biological effects of curcumin and its role in cancer chemoprevention and therapy. *Anticancer Agents Med Chem*, 6(3), 259-270.
- Singh, S. V., Hu, X., Srivastava, S. K., Singh, M., Xia, H., Orchard, J. L., et al. (1998). Mechanism of inhibition of benzo[a]pyrene-induced forestomach cancer in mice by dietary curcumin. *Carcinogenesis*, 19(8), 1357-1360.
- Smith, B., Wise, S., Vogt, A., Nakashima, M., Herber, R., & Hulkower, K. (2008). Substrate Dependent Effects of c-Met Inhibitors on HGF-induced Cell Migration. A Snapshot of Lung Cancer. (2009). 2010(4/16/2010). Retrieved from <http://www.cancer.gov/aboutnci/servingpeople/snapshots/lung.pdf>
- Soderholm, J., & Heald, R. (2005). Scratch n' screen for inhibitors of cell migration. *Chem Biol*, 12(3), 263-265.
- Solan, N. J., Miyoshi, H., Carmona, E. M., Bren, G. D., & Paya, C. V. (2002). RelB cellular regulation and transcriptional activity are regulated by p100. *J Biol Chem*, 277(2), 1405-1418.
- Somasundaram, S., Edmund, N. A., Moore, D. T., Small, G. W., Shi, Y. Y., & Orłowski, R. Z. (2002). Dietary curcumin inhibits chemotherapy-induced apoptosis in models of human breast cancer. *Cancer Res*, 62(13), 3868-3875.
- Soni, K. B., & Kuttan, R. (1992). Effect of oral curcumin administration on serum peroxides and cholesterol levels in human volunteers. *Indian J Physiol Pharmacol*, 36(4), 273-275.
- South, E. H., Exon, J. H., & Hendrix, K. (1997). Dietary curcumin enhances antibody response in rats. *Immunopharmacol Immunotoxicol*, 19(1), 105-119.
- Sreejayan, & Rao, M. N. A. (1997). Nitric oxide scavenging by curcuminoids. *Journal of Pharmacy and Pharmacology*, 49(1), 105-107.
- Srinivasan, M. (1972). Effect of curcumin on blood sugar as seen in a diabetic subject. *Indian J Med Sci*, 26(4), 269-270.
- Srivastava R, D. M., Srimal RC, Dhawan BN. (1985). Antithrombotic effect of curcumin. 40, 413-417.
- Stetler-Stevenson, W. G. (1999). Matrix metalloproteinases in angiogenesis: a moving target for therapeutic intervention. *J Clin Invest*, 103(9), 1237-1241.

- Sun, C., Liu, X., Chen, Y., & Liu, F. (2005). Anticancer effect of curcumin on human B cell non-Hodgkin's lymphoma. *J Huazhong Univ Sci Technolog Med Sci*, 25(4), 404-407.
- Syng-Ai, C., Kumari, A. L., & Khar, A. (2004). Effect of curcumin on normal and tumor cells: role of glutathione and bcl-2. *Mol Cancer Ther*, 3(9), 1101-1108.
- Tayyem, R. F., Heath, D. D., Al-Delaimy, W. K., & Rock, C. L. (2006). Curcumin content of turmeric and curry powders. *Nutr Cancer*, 55(2), 126-131.
- Thakur, R., Puri, H. S. and Husain, A. (1989). Major medicinal plants of India. *Central Institute of Medicinal and Aromatic Plants, Lucknow*.
- Thaloor, D., Singh, A. K., Sidhu, G. S., Prasad, P. V., Kleinman, H. K., & Maheshwari, R. K. (1998). Inhibition of angiogenic differentiation of human umbilical vein endothelial cells by curcumin. *Cell Growth Differ*, 9(4), 305-312.
- Thomas-Eapen, N. E. (2009). Turmeric: the intriguing yellow spice with medicinal properties. *Explore (NY)*, 5(2), 114-115.
- Tilak, J. C., Banerjee, M., Mohan, H., & Devasagayam, T. P. (2004). Antioxidant availability of turmeric in relation to its medicinal and culinary uses. *Phytother Res*, 18(10), 798-804.
- Tomita, M., Holman, B. J., Santoro, C. P., & Santoro, T. J. (2005). Astrocyte production of the chemokine macrophage inflammatory protein-2 is inhibited by the spice principle curcumin at the level of gene transcription. *J Neuroinflammation*, 2(1), 8.
- Tsuji, T., Ibaragi, S., & Hu, G. F. (2009). Epithelial-mesenchymal transition and cell cooperativity in metastasis. *Cancer Res*, 69(18), 7135-7139.
- Tsuji, T., Ibaragi, S., Shima, K., Hu, M. G., Katsurano, M., Sasaki, A., et al. (2008). Epithelial-mesenchymal transition induced by growth suppressor p12CDK2-AP1 promotes tumor cell local invasion but suppresses distant colony growth. *Cancer Res*, 68(24), 10377-10386.
- Tsvetkov, P., Asher, G., Reiss, V., Shaul, Y., Sachs, L., & Lotem, J. (2005). Inhibition of NAD(P)H:quinone oxidoreductase 1 activity and induction of p53 degradation by the natural phenolic compound curcumin. *Proc Natl Acad Sci U S A*, 102(15), 5535-5540.
- Urbina-Cano, P., Bobadilla-Morales, L., Ramirez-Herrera, M. A., Corona-Rivera, J. R., Mendoza-Magana, M. L., Troyo-Sanroman, R., et al. (2006). DNA damage in mouse lymphocytes exposed to curcumin and copper. *J Appl Genet*, 47(4), 377-382.
- Vajragupta, O., Boonchoong, P., Watanabe, H., Tohda, M., Kummasud, N., & Sumanont, Y. (2003). Manganese complexes of curcumin and its derivatives: evaluation for the radical scavenging ability and neuroprotective activity. *Free Radic Biol Med*, 35(12), 1632-1644.
- Venkatesan, N. (1998). Curcumin attenuation of acute adriamycin myocardial toxicity in rats. *Br J Pharmacol*, 124(3), 425-427.
- Vilimas, T., Mascarenhas, J., Palomero, T., Mandal, M., Buonamici, S., Meng, F., et al. (2007). Targeting the NF-[kappa]B signaling pathway in Notch1-induced T-cell leukemia. [10.1038/nm1524]. *Nat Med*, 13(1), 70-77.
- Wahlstrom, B., & Blennow, G. (1978). A study on the fate of curcumin in the rat. *Acta Pharmacol Toxicol (Copenh)*, 43(2), 86-92.

- Wang, X., Belguise, K., Kersual, N., Kirsch, K. H., Mineva, N. D., Galtier, F., et al. (2007). Oestrogen signalling inhibits invasive phenotype by repressing RelB and its target BCL2. *Nat Cell Biol*, 9(4), 470-478.
- Wang, Y. J., Pan, M. H., Cheng, A. L., Lin, L. I., Ho, Y. S., Hsieh, C. Y., et al. (1997). Stability of curcumin in buffer solutions and characterization of its degradation products. *J Pharm Biomed Anal*, 15(12), 1867-1876.
- What You Need to Know About Lung Cancer. (2007). (Vol. 2010): National Institutes of Health.
- Xiao, H., Xiao, Q., Zhang, K., Zuo, X., & Shrestha, U. K. (2010). Reversal of multidrug resistance by curcumin through FA/BRCA pathway in multiple myeloma cell line MOLP-2/R. *Ann Hematol*, 89(4), 399-404.
- Xu, Y., Pindolia, K., Janakiraman, N., Chapman, R. and Gautam, S. (1998). Curcumin inhibits IL-1alpha and TNFalpha induction of AP-1 and NFkB DNA-binding activity in bone marrow stromal cells. *Hematopathol. Mol. Hematol*.
- Yang, J., Mani, S. A., Donaher, J. L., Ramaswamy, S., Itzykson, R. A., Come, C., et al. (2004). Twist, a master regulator of morphogenesis, plays an essential role in tumor metastasis. *Cell*, 117(7), 927-939.
- Yang, J., Pan, W. H., Clawson, G. A., & Richmond, A. (2007). Systemic targeting inhibitor of kappaB kinase inhibits melanoma tumor growth. *Cancer Res*, 67(7), 3127-3134.
- Yarrow, J. C., Perlman, Z. E., Westwood, N. J., & Mitchison, T. J. (2004). A high-throughput cell migration assay using scratch wound healing, a comparison of image-based readout methods. *BMC Biotechnol*, 4, 21.
- Yoshino, M., Haneda, M., Naruse, M., Htay, H. H., Tsubouchi, R., Qiao, S. L., et al. (2004). Prooxidant activity of curcumin: copper-dependent formation of 8-hydroxy-2'-deoxyguanosine in DNA and induction of apoptotic cell death. *Toxicol In Vitro*, 18(6), 783-789.
- Zahm, J. M., Kaplan, H., Herard, A. L., Doriot, F., Pierrot, D., Somelette, P., et al. (1997). Cell migration and proliferation during the in vitro wound repair of the respiratory epithelium. *Cell Motil Cytoskeleton*, 37(1), 33-43.
- Zetter, B. R. (1993). Adhesion molecules in tumor metastasis. *Semin Cancer Biol*, 4(4), 219-229.
- Zou, P., Kawada, J., Pesnicak, L., & Cohen, J. I. (2007). Bortezomib induces apoptosis of Epstein-Barr virus (EBV)-transformed B cells and prolongs survival of mice inoculated with EBV-transformed B cells. *J Virol*, 81(18), 10029-10036.

APPENDIX

Optimized Protocol

1. The Oris 95-well plate was removed from storage at 4°C and allowed to equilibrate at room temperature for approximately 1 hour.
2. The bottom of the plate was visually inspected to ensure that all the Cell Seeding Stoppers are firmly sealed against the bottom of the plate. Specifically the plate was be tipped at an angle and viewed under indirect light to reveal the “bullseye” pattern at the bottom of the well.
3. Cells were trypsinized and counted and the suspension was prepared that is 10-fold greater in density than the optimal seeding concentration.
 - a. The optimal cell density for the A549 is 60,000 cells/well
4. 100ul of suspended cells was pipetted into each well, being careful not to disturb the Cell Seeding Stoppers or the well coatings upon the introduction of the pipette tip, specifically by placing the pipette tip along the wall of the well.
5. The plate was lightly tapped to ensure even distribution of well contents.
6. The seeded plate was incubated in a humidified chamber (37C, 5% CO₂) overnight to permit cell attachment.
7. The following day the plate was removed from the incubator and cell growth was visually inspected with an inverted microscope to ensure 90% confluency was reached at the perimeter of the detection zone.
8. The Oris Stopper tool was rinsed with 70% ethanol. Stoppers were then removed from the all the wells with the Stopper Tool, except wells denoted as “reference wells.” In reference wells stoppers remained in place for the entire duration of the experiment. The plate was secured by firmly pressing it down against the work surface. The tines of the Stopper Tool were slid underneath the back bone of the stopper strip. The Stopper Tool was then lifted slowly in the vertical direction to gently remove the stoppers and to avoid splashing of the well contents.
9. Media was removed from the wells by inverting the plate and dumping out contents,
10. Wells were then gently washed 100ul of sterile PBS to remove any unattached or “rogue” cells. Pipetting was used to aliquot PBS into wells while PBS was removed by inverting the plate.
11. 100ul of fresh media will be added following the wash.
12. Drugs were diluted to the appropriate concentrations at a final volume of 1μL, and pipetted into wells

13. Four hours later, 10 ng/mL TNF- α was added to each well.
14. The plate was incubated in a humidified chamber for 72hrs to allow for migration.
15. After 72 hours the plate was inverted and contents were dumped out.
16. Wells were fixed in 2% para-formaldehyde and stained with 1:5000 dilution of Hoechst 33258.
17. The plate was be imaged using the IXMicro5000, both with and without the application of the detection mask.
18. Various analyses were be run after imaging was complete using ImageJ and Meta Xpress Software.

1